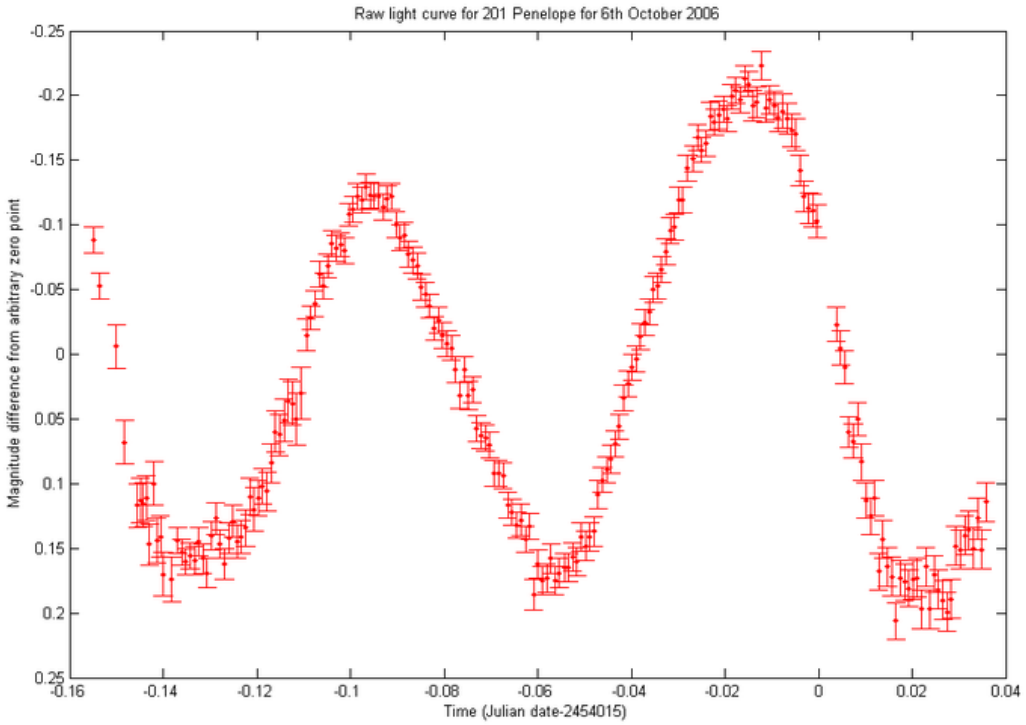
Asteroid Light Curves

Asteroid research can include new discoveries, orbits, diameters, spin rates, pole direction, mass, composition, geometric albedo measurements, and more. Much of the current research contains large amounts of estimates and needs more data. Some of the parameters can be inferred from one data set, some need multiple data sets from several instrument and telescope types. Ground based telescopes have been heavily utilized in the collection of asteroid data. Space based telescopes are often coupled with ground based observations to try and complete data sets.

The goal of this project is to measure light curves of asteroids, making sure to have sufficient exposure time for good measurements in addition to sampling frequently enough for the typical few hour rotation period of a typical asteroid. Some objects have very good light curves; some don't have any light curves at all. Below is an example light curve for 201 Penelope (an asteroid discovered in 1879). Even on an asteroid that has been researched as long as Penelope, it still has a lot of missing morphological data.



Example Light Curve for Asteroid 201 Penelope (Mount John University Observatory)

Targets

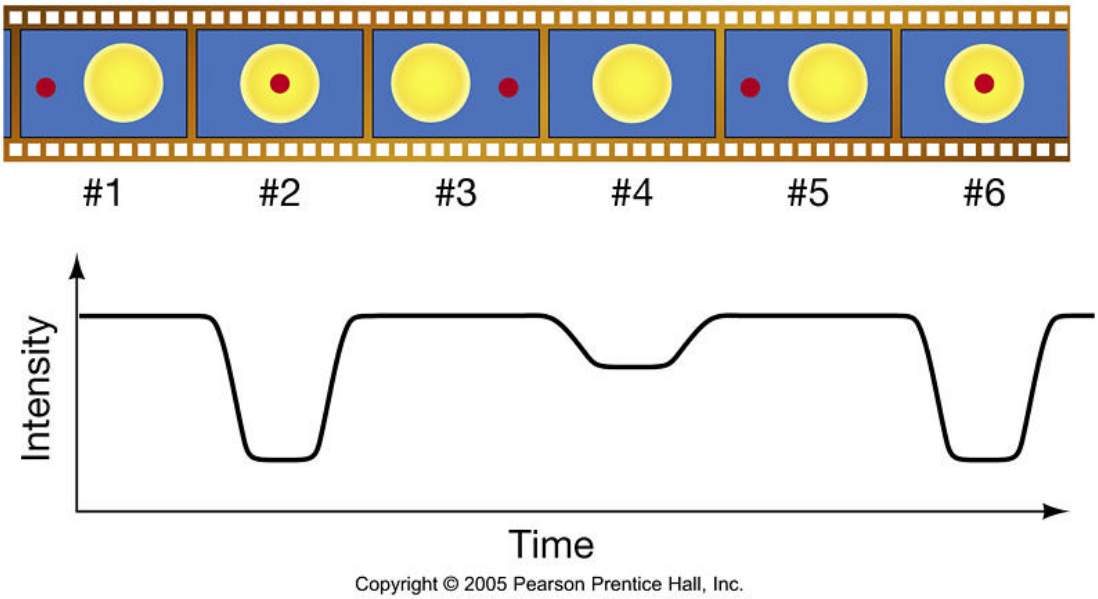
Name	RA (J2000)	DEC (J2000)	APmag
44 Nysa	13 42 38.08	-07 54 08.8	11.4
42 Isis	10 56 01.06	+13 32 35.8	13.6
35 Leukothea	14 22 55.27	-19 00 22.2	13.7
41 Daphne	14 23 30.26	-06 18 14.0	12.0
198343 (2004 VG)	00 19 10.33	+15 52 30.3	19.2
17 Thetis	11 42 02.38	+04 42 51.8	13.2
70 Panopaea	17 13 10.40	-31 09 48.9	12.9
203247 (2001 QK6)	15 05 22.42	-03 12 38.7	21.9
46 Hestia	01 59 07.28	+10 03 24.5	10.8
2 Pallas	01 14 08.70	-16 40 36.5	8.3
73 Klytia	09 27 32.77	+17 05 06.1	14.4
929 Algunde	08 29 57.77	+15 51 05.8	16.7
4902 Thessandrus	12 49 12.64	-02 25 51.4	17.7
433 Eros	16 27 01.88	-25 59 11.6	14.1
42981 Jenniskens	16 15 19.29	-17 16 34.1	20.7
1 Ceres	07 25 39.49	+23 31 06.5	8.5
203046 (2000 EC45)	09 40 22.19	+25 23 24.6	20.7
2650 Elinor	15 34 03.13	-30 16 34.9	16.8
6 Hebe	09 32 19.24	+10 18 36.1	10.7
281375 (2008 JV19)	12 21 53.88	-00 53 33.8	22.7
2009 BD81	19 40 21.51	-28 26 11.4	26.2
69 Hesperia	15 10 13.34	-12 15 55.3	13.3
123 Brunhild	17 14 12.12	-25 59 04.0	14.9
130 Elektra	09 13 01.91	+06 52 16.4	13.4
8 Flora	19 24 23.70	-24 57 28.7	10.7
7 Iris	13 27 50.00	-12 46 46.1	11.1
139 Juewa	19 49 11.75	-29 57 34.7	13.8

Note: Positions are for UT 2026-10-17 05:00

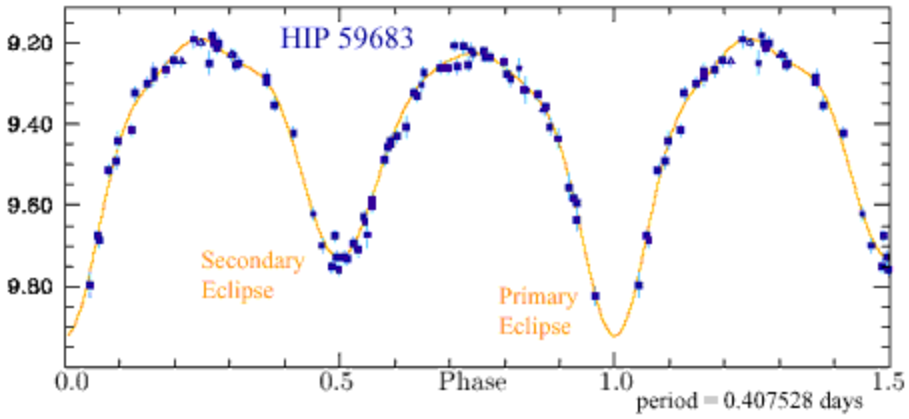
Ephemeris Generators
http://ssd.jpl.nasa.gov/horizons/app.html

Binary Stars (Eclipsing) Light Curves

Binary stars are extremely valuable for astronomical research. They provide significant amounts fundamental information about star formation (the study of Algol and the Algol Paradox, for example, gave to rise to the idea of mass transfer). One of the elemental aspects of binary star research is collecting light curves. Light curves can yield orbital periods and relative sizes of the stars. Our goal is to obtain light curves for the objects below.



Visual representation of a eclipsing binary's light curve.



HIP 59683's Light Curve (credit -ESA)

Targets

Object	RA (J2000)	DEC (J2000)	Mag	Period (days)
MACHO 211.16590.1434	01 00 01	-73 11 29	20.08	1.26
GSC 0619-0232	01 18 48	+13 21 08	14.3	0.25
Algol (Beta Per)	03 08 10	+40 57 20	2.2	2.1
YY Eri	04 12 09	-10 28 10	8	0.3215
GSC 1848-1264	05 30 19	+23 51 27	11.02	0.3478
GSC 2936 0478	06 35 41	+42 00 15	13.8	0.4388
HD 65498	08 00 46	+42 10 33	9.7	1.3
HD 67894	08 11 54	+42 54 36	9.98	0.3
GSC 0804-0118	08 31 25	+11 48 13	14.2	0.3237
W Uma	09 43 46	+55 57 09	8	0.25
BD+20 2890	13 53 53	+20 09 43	10.4	0.5
GSC 03472-00641	14 21 44	+46 41 59	11.4	0.3

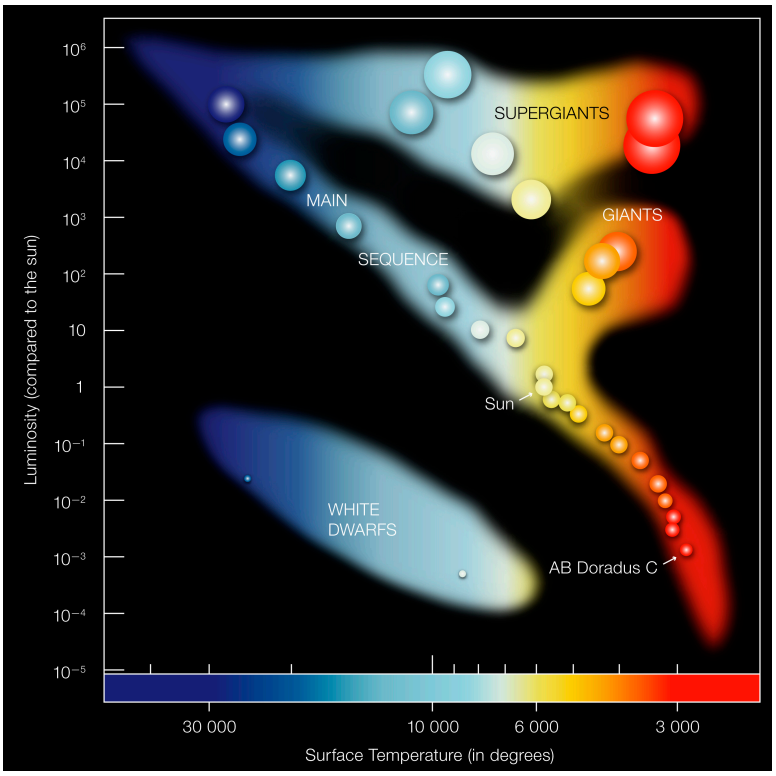
http://www.aavso.org/ - American Association of Variable Star Observers

Cluster Colour-Magnitude Diagrams

For this project you will observe open and/or globular clusters in order to construct Colour-Magnitude diagrams (CMDs) and identify the evolutionary sequences.

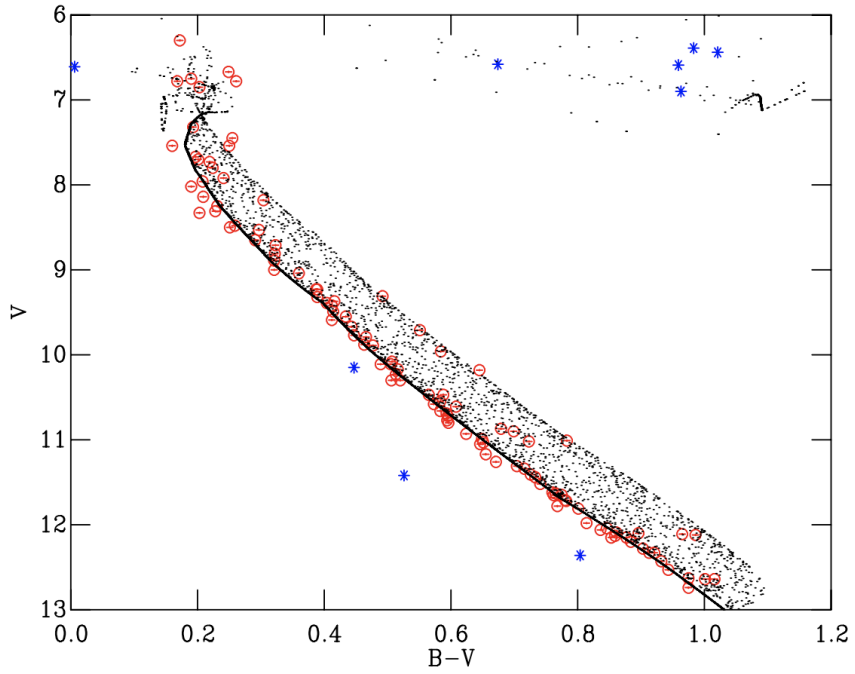
Stars are 'born' from clumps of gas, which collapse under gravity to form dense pre-stellar cores. As these cores continue to collapse, the temperature and luminosity increases until eventually the temperature and pressure in the center is sufficient for hydrogen fusion to begin. When fusion begins, the star becomes stable against further collapse.

The Hertzsprung-Russell (HR) diagram is a plot of luminosity vs temperature. In an HR diagram, stable hydrogen-burning stars fall along a tight line called the Main Sequence. Young proto-stars are still collapsing towards the main sequence, and older, evolved stars have turned off the main sequence.



An example HR Diagram, showing the main sequence, Giant and Supergiant branches, and white dwarfs. (Credit: ESO)

By placing stars in this diagram we are able to determine their state of evolution. If we were able to directly observe temperature and luminosity in



A CMD for the open cluster Praesepe. Red and blue points show stars in Praesepe. Overlaid in black is a model population. Note the blue points in the upper right, which are stars evolving off the main sequence.

stars this would be straightforward. However we are not able to directly observe temperature or luminosity. Instead we construct Colour Magnitude Diagrams (CMDs). We plot a stars magnitude against its colour (the difference between two magnitudes in different filters). Magnitude is a proxy for luminosity, and colour is a proxy for temperature (hotter stars are more blue, cool stars are more red).

Clusters are ideal targets for constructing CMDs. Because the stars in a cluster all reside at a common distance we can (mostly) neglect the effect of distance and extinction. We can also discount metallicity effects due to the clusters assumed shared origins. Globular clusters are massive, dense collections of old stars, while open clusters are smaller groups of much younger stars. Thus if you observe a globular cluster its CMD will be very different from that of an open cluster. Additionally, consider that open clusters can cover large areas on the sky, and so you may need multiple exposures to cover enough cluster members to create a CMD.

Open and Globular clusters

Open Clusters					
Object	RA (J2000)	Dec (J2000)	V Mag	Age (Gyr)	Distance (pc)
Blanco 1	00 04 24.0	-29 56 24.0	10-19	0.13	251
χ Per	02 22 48.7	+57 07 30.0	7-23	0.014	916
IC 348	03 44 34	+32 09 46.8 11.	13-22	0.006	249
Pleiades	03 47 00	+24 07 01.2	4-22	0.13	133
λ Ori	05 36 25.0	+09 38 25.8	3-22	0.010	402
σ Ori	05 40 14.2	-02 20 18.0	6.5-23	0.006	407
NGC 2169	06 08 24.0	+13 57 54.0	7-23	0.011	995
NGC 2244	06 31 55.5	+04 56 34.3	6-22	0.002	1380
NGC 2264	06 39 47.1	+09 53 36.8	12-20	0.004	776
NGC 2362	07 18 36.5	-24 57 00.0	8-21	0.012	1318
Praesepe	08 40 24	+19 40 01.2	6-23	0.66	184
Chamaeleon 1	11 08 20.0	-77 00 00.0	10-20	0.006	160
Coma Ber	12 23 13.5	+26 02 18.3	6-17	0.562	86
Sco-Cen	16 04 17.91	-19:41:51.08	7-18	0.002	96
ρ Oph	16 26 48.0	-24 26 48.0	8-18	0.008	120
NGC 6530	18 04 05.0	-24 22 00.0	5-21	0.002	1343
NGC 6611	18 18 48.0	-13 47 00.0	6-22	0.002	1888
IC 5146	21 53 24.0	+47 15 36.0	14-22	0.002	916
NGC 7160	21 53 40.0	+62 36 12.0	5-21	0.014	859
Cep OB3b	22 55 43.3	+62 40 13.6	4.5-23	0.006	570
Globular Clusters					
Object	RA (J2000)	Dec (J2000)	V Mag	Age (Gyr)	Distance (pc)
47 Tuc	00 24 05.36	-72 04 53.2	12-22	13.06	4000
Omega Cen	13 26 47.28	-47 28 46.1	13-22	13.5	5470
NGC 6402	17 37 36.10	-03 14 45.3	15-22	10.9	9300
NGC 6584	18 18 37.6	-52 12 56.8	14-21	11	14000
NGC 6981	20 53 27.7	-12 32 14.3	14-20	9.5	16730
NGC 7078	21 29 58.3	+12 10 01	14-24	12.7	10230
NGC 7089	21 33 29.3	-00 49 23	13-23	13.0	17000
Balbinot 1	22 10 43.15	14 56 58.8	18-22	11.7	31900

Comparative Visual Inspection Spectroscopy[1]

Spectroscopy is one of the most powerful techniques at astronomers disposal. The technique of probing the light from remote sources provides a wealth of information about the chemistry (e.g. isotopic abundances) and physics (e.g. temperatures, dynamics, magnetic fields) of both remote objects and environments along the intervening line of sight. Many astronomical sources are categorized on the basis of their spectra (e.g. the strength of various lines in stellar spectral archetypes, O, B, A, F, G, K, M, etc.; discrimination between types of supernova; serendipetous detection of 'exotic' objects such as Be stars, Carbon stars and Diffuse Interstellar Band, DIB sources).

A candidate list of somewhat 'exotic' stellar objects (many of which were first investigated with Lick Observatory facilities) follows. With supposedly vastly differing spectral features discrimination between sources should be self evident from comparitive visual inspection of raw, unprocessed data. The following list should be considered as a starting point, upon which to design a half-night observing campaign, ensuring a broad range of differing types of source.

On-line resources (e.g. Simbad, Visier, NED) can also be consulted to add other exotic sources as well as comparison sources.

References

A general catalogue of galactic carbon stars by C.B. Stephenson. Third edition. Alksnis et al., 2001, Baltic Astronomy, **10**, 1.

Bright Stars. The Astronomical Almanac. Taunton: The United Kingdom Hydrographic Office.

A library of Stellar Spectra. Jacoby et al., 1984, ApJS, **56**, 257.

A catalog of Be Stars. Jaschek, M. & Egret, D., 1982, IAU, **98**, 261.

The Diffuse Interstellar Bands. Herbig, G., 1995, ARAA, **33**, 19.

Diffuse Interstellar Bands. IV. McCall, B.J., et al. 2010, ApJ, **708**, 1628.

Spectroscopically Identified White Dwarfs. McCook, G.P., et al. 2008, ApJS **121**, 1.

An Atlas of Stellar Spectra. With an Outline of Spectral Classification. Morgan, W., Keenan, P. & Kellman, E., 1943, University of Chicago Press.

Spectral Classification. Morgan, W. & Keenan, P., ARAA, 11, **29**.

[1]Developed by 2012 UCO/Lick Summer intern, Megan Clendenin (UCD).

Identifier	R.A.	Dec.	Equinox	V(?)	Description
Beta Cass	00 09 51.1	+59 13 07	2012.5	2.27	Bright Star, F2III
MWC 8	00 41 55.6	+48 00 38	1950.0	4.54	Be Star, B5III
Gamma Cass	00 56 42.5	+60 43 00.3	2000.0	2.47	Be Star
HD 6327.	01 05 23.0	+60 25 19	2000.0	11.33	Wolf-Rayet Star
0116+2546	01 16 05.0	+25 46 10	2000.0	6.70	Carbon Star
R Scl.	01 26 59.0	−32 32 44	2000.0	6.1	Carbon Star
HD 9612.	01 33 13.1	+74 02 46	1950.0	6.4	Be Star, B9V
Alpha Ari	02 07 52.9	+23 31 16	2012.5	2.0	Bright Star, K2III
MWC 455	03 00 11.7	+38 07 54	2000.0	5.9	Be Star, B8V
HD 23180	03 44 19.1	+32 17 17.7	2000.0	3.85	DIB, B1III
Xi Per	03 59 46.8	+35 49 34	2012.5	4.04	Bright Star, O7.5III
WD 0413-077	04 15 21.0	−07 39 30	2000.0	9.52	White Dwarf
HD 30614	04 54 03.0	+66 20 33.6	2000.0	4.3	DIB, O9.5I
CGCS 833	04 59 36.3	−14 48 23.0	2000.0	5.9	Carbon Star
119 Tauri	05 32 12.7	+18 35 39.2	2000.0	4.37	M2I star
M42, Orion Neb	05 35 17.3	−05 23 28	2000.0	5.0	HII (ionized) region
MWC 115	05 37 38.6	+21 08 33	2000.0	3.0	Be Star, B2III
Sirius B	06 45 09.0	−16 43.1	2000.0	8.3	White Dwarf
HD 50896	06 54 13.0	−23 55 42	2000.0	6.74	Wolf-Rayet Star
HD 54662	07 09 20.3	−10 20 47.6	2000.0	6.2	DIB, O7III
MWC 178	07 27 09.2	+08 17 22	2000.0	2.9	Be Star, B8V
Procyon B	07 39 19.7	+05 15 25	2000.0	10.92	White Dwarf
WD 0839-327.	08 41 31.0	−32 56.3	2000.0	11.9	White Dwarf
CGCS 2378	08 55 22.9	+17 13 53	2000.0	6.1	Carbon Star
Epsilon Leo	09 46 33.5	+23 42 58	2012.5	2.98	Bright Star, G1II
MWC 205	10 30 59.9	−13 35 17	2000.0	5.6	Be Star, B9V
HD 91316	10 32 48.7	+09 18 23.7	2000.0	3.87	DIB, B1I
HD 100673.	11 34 45.8	−54 15 51	2000.0	4.62	Be Star, B9V
CGCS 3283	12 45 07.8	+45 26 25	2000.0	4.8	Carbon Star
BY Boo	14 08 25.7	+43 47 43	2012.5	5.27	Bright Star, M4.5III
MWC 237	15 32 55.8	+31 21 32	2000.0	4.1	Be Star, B6V
V Crb	15 49 31.2	+39 34 16	2000.0	6.9	Carbon Star
HD 149757	16 37 09.5	−10 34 1.5	2000.0	2.6	DIB, 09.5V
HD 165763	18 08 28.5	−21 15 11.2	2000.0	7.68	Wolf-Rayet Star
CGCS 4121	18 50 20.0	−07 54 27	2000.0	6.3	Carbon Star
HD 179406	19 12 40.7	−07 56 22.3	2000.0	5.36	DIB, B3V
HD 183143	19 27 26.6	+18 17 45.2	2000.0	6.9	DIB
WD 1944-421.	19 47 40.0	−42 00.6	2000.0	10.4	White Dwarf
HD 190918	20 05 57.3	+35 47 18.1	2000.0	6.8	Wolf-Rayet Star
MWC 329	20 09 25.5	+36 50 20	2000.0	4.9	Be Star, B2V
HD 192163	20 12 06.5	+38 21 17.7	2000.0	7.48	Wolf-Rayet Star
CGCS 4758	20 13 23.7	+38 43 45	2000.0	6.5	Carbon Star
HD 208440	21 53 53.3	+62 36 00.7	2000.0	7.9	DIB, B1V
MWC 388	22 25 16.5	+01 22 37	2000.0	4.66	Be Star, B1V
CGCS 5928	23 46 23.5	+03 29 13	2000.0	5.3	Carbon Star

The Search for Extra-Solar Planets

This project involves using the radial velocity method to search for extra-solar planets around nearby sub-giant stars. The method relies upon being able to accurately measure Doppler shifts of a group of spectral lines in the spectra of the star. This requires the use of high resolution spectroscopy. In addition an accurate knowledge of the time of observation is required.

The goal of this exercise is to acquire the high resolution spectra of the candidate stars that are required to enable an accurate determination of their radial velocities. The result of one night of observation is one point on a radial velocity curve for each target observed (see Figure 1). Follow up observations carried out over many months or even years are required in order to obtain a complete radial velocity curve for each target. Subsequent analysis of these radial velocity curves are used to deduce the presence of extra-solar planets and derive their orbital elements.

Targets

Name	RA(J2000)	Dec(J2000)	V
HD 143761	16 01 02.3	+33 17 58	5.4
HD 165438	18 06 15.3	-04 45 05	5.7
HD 168723	18 21 17.8	-02 54 09	3.3
HD 173667	18 45 39.7	+20 32 40	4.2
HD 185395	19 36 27.0	+50 13 15	4.5
HD 186408	19 41 48.6	+50 31 27	6.0
HD 186427	19 41 51.6	+50 31 00	6.2
HD 208801	21 58 54.9	-04 22 28	6.2
HD 215648	22 46 41.8	+12 10 13	4.2
HD 217014	22 57 28.2	+20 46 09	5.5
HD 217107	22 58 15.5	-02 23 44	6.2
HD 400	00 08 40.7	+36 37 35	6.2
HD 6706	01 07 46.4	-09 47 08	5.7
HD 8673	01 26 09.1	+34 34 45	6.3
HD 9826	01 36 47.5	+41 24 12	4.1
HD 10700	01 44 01.7	-15 55 58	3.5
HD 11151	01 50 57.2	+51 55 58	6.0
HD 16160	02 36 07.2	+06 53 41	5.8
HD 16895	02 44 12.6	+49 13 41	4.1
HD 19373	03 09 06.5	+49 36 46	4.1
HD 19994	03 12 46.6	-01 11 47	5.1
HD 20630	03 19 22.0	+03 22 15	4.8
HD 22049	03 32 54.5	-09 27 29	3.7
HD 22484	03 36 52.0	+00 23 57	4.3
HD 26965	04 15 13.4	-07 40 16	4.4
HD 30495	04 47 36.4	-16 56 01	5.5

Name	RA(J2000)	Dec(J2000)	V
HD 30562	04 48 36.7	-05 40 31	5.8
HD 30652	04 49 51.0	+06 57 41	3.2
HD 32923	05 07 27.7	+18 38 43	5.0
HD 33555	05 10 58.1	-02 15 18	6.2
HD 34411	05 19 09.3	+40 05 44	4.7
HD 38529	05 46 34.8	+01 10 03	5.9
HD 39587	05 54 22.7	+20 16 32	4.4
HD 43042	06 14 50.7	+19 09 20	5.2
HD 48682	06 46 44.3	+43 34 42	5.3
HD 52711	07 03 30.6	+29 19 58	5.9
HD 55575	07 15 50.1	+47 14 20	5.6
HD 69830	08 18 24.3	-12 38 15	5.9
HD 69897	08 20 03.8	+27 12 56	5.1
HD 71148	08 27 36.7	+45 39 04	6.3
HD 75732	08 52 35.1	+28 19 46	5.9
HD 76151	08 54 17.4	-05 26 03	6.0

Rapidly Rotating B Stars for calibration purposes

Name	RA(J2011.5)	Dec(J2011.5)	V
HR 804	02 43 53.9	03 17 01	3.4
HR 1165	03 48 10.2	24 08 24	2.8
HR 1251	04 03 46.2	06 01 14	3.9
HR 1998	05 47 28.6	-14 49 06	3.5
HR 2421	06 38 22.5	16 23 18	1.9
HR 2618	06 59 04.7	-28 59 18	1.5
HR 3314	08 26 14.1	-03 56 40	3.9
HR 3594	09 04 24.3	47 06 37	3.6
HR 3665	09 14 57.7	02 15 55	3.8
HR 3690	09 19 33.4	36 45 12	3.8
HR 4033	10 17 47.1	42 51 23	3.4
HR 5107	13 35 16.8	00 39 15	3.3
HR 5812	15 39 21.9	-29 48 53	3.6
HR 5867	15 46 43.1	15 23 11	3.6
HR 5881	15 50 13.3	-03 27 53	3.5
HR 5928	15 57 35.8	-29 14 49	3.8
HR 6165	16 36 36.0	-28 14 20	2.8
HR 6324	17 00 43.8	30 54 36	3.9
HR 6629	17 48 28.2	02 42 13	3.7
HR 7039	18 46 22.5	-26 58 41	3.1
HR 7121	18 55 58.7	-26 16 53	2.0
HR 7178	18 59 22.4	32 42 21	3.2
HR 7194	19 03 20.6	-29 51 46	2.6
HR 7235	19 05 56.3	13 52 53	2.9

Name	RA(J2011.5)	Dec(J2011.5)	V
HR 7236	19 06 51.5	-04 51 52	3.4
HR 7528	19 45 20.0	45 09 34	2.8
HR 7710	20 11 53.9	00 47 12	3.2
HR 7906	20 40 10.3	15 57 12	3.7
HR 8028	20 57 36.2	41 12 43	3.9
HR 8634	22 42 02.2	10 53 30	3.4
HR 8709	22 55 15.6	-15 45 34	3.2

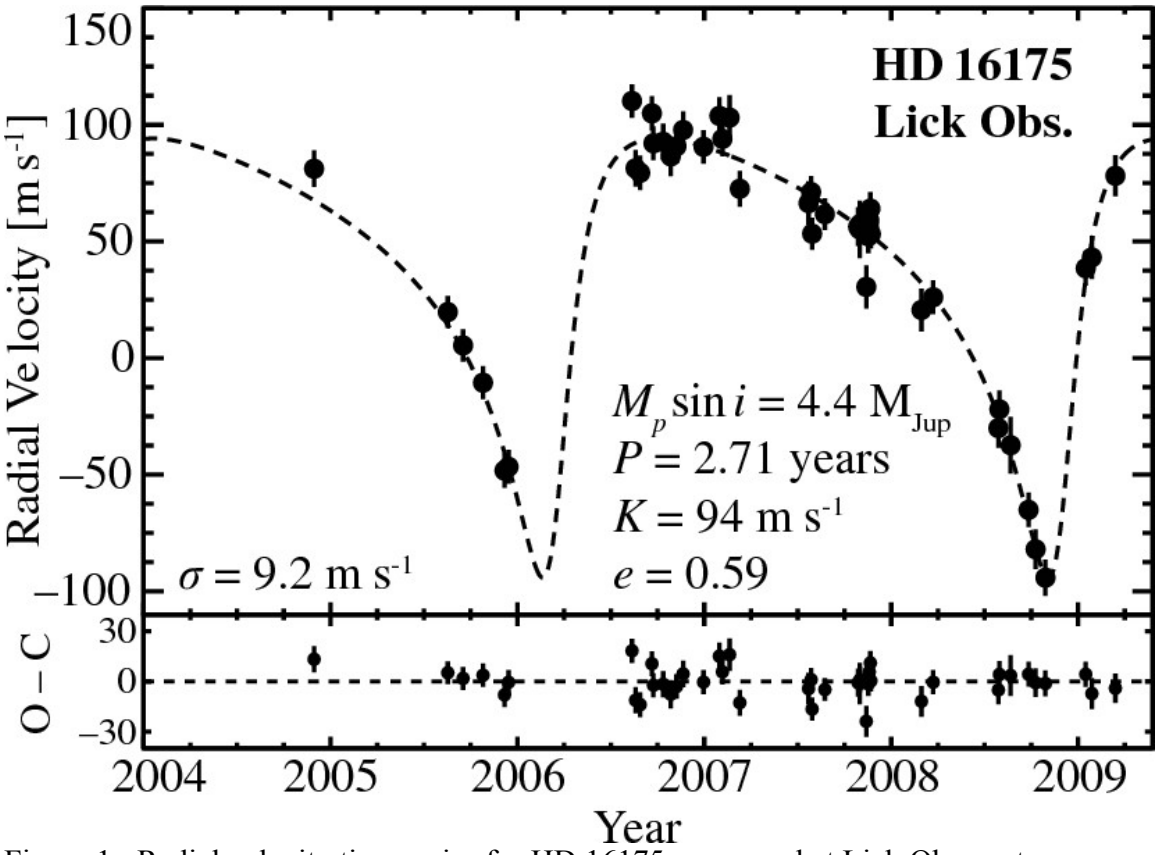


Figure 1: Radial velocity time series for HD 16175, measured at Lick Observatory. (Peek, et al. 2009 PASP 121:613)

Rotation Curves

The rotation of spiral galaxies does not match that expected according to Keplerian dynamics, as originally demonstrated by Louise Volders' (1959) observations of spiral galaxy M33. This discrepancy was later attributed to the presence of dark matter by Vera Rubin.

We plan to observe edge-on spiral galaxies to measure their rotation rates as a function of radius. From this we will determine the proportion of dark matter in each galaxy. Typical rotation velocities tend to be 100's km/s.

PA is the position angle of the major axis in degrees east of north. MajA (MinA) is the major (minor) axis dimension in arcminutes. Btot is the total integrated B magnitude of the galaxy.

Potential Targets:

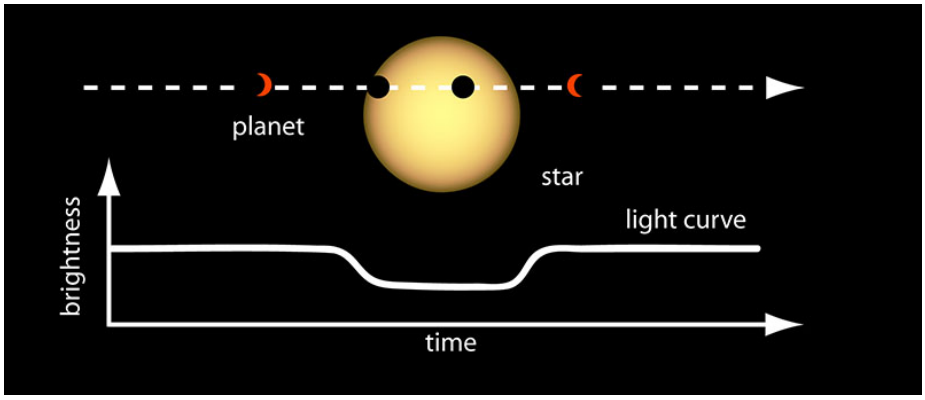
Name	RA(2000)	Dec(2000)	PA (Deg)	MajA (arcmin)	MinA	Btot mag
PGC124	00 01 36.8	+03 30 17	3	1.34	0.17	16.0
FGC136	01 10 36.0	-29 48 00	115	0.60	0.08	17.2
PGC6699	01 49 31.4	+32 35 20	38	5.82	0.65	13.3
PGC7933	02 04 55.4	+43 09 18	118	1.57	0.15	15.9
FGC400	03 15 03.6	+16 12 58	38	0.72	0.09	17.1
PGC14600	04 10 33.1	-07 10 00	66	2.20	0.22	15.2
PGC15967	04 46 15.8	+76 25 08	74	4.59	0.63	13.8
FGC493	05 24 30.4	-37 35 30	147	0.73	0.08	17.0
PGC19281	06 35 02.4	-19 27 47	155	1.72	0.17	15.8
FGC676	07 46 24.5	-65 49 28	134	0.53	0.05	18.1
PGC22446	08 00 23.5	+42 11 32	8	2.52	0.34	14.8
PGC25886	09 10 49.4	-08 53 22	32	6.50	0.69	13.2
PGC30487	10 24 07.2	-05 37 56	72	1.57	0.20	15.5
PGC32550	10 51 24.0	-19 53 24	151	4.26	0.48	14.0
FGC854	11 03 02.5	-39 02 06	47	0.47	0.05	18.0
PGC38567	12 08 42.0	+36 48 11	83	5.21	0.67	13.5
PGC38988	12 13 17.5	+43 41 52	165	6.27	0.67	13.3
PGC39422	12 17 30.0	+37 48 31	48	19.38	2.13	10.2
PGC45084	13 03 17.0	-17 25 23	115	8.01	1.06	12.5
PGC47394	13 29 48.7	-17 57 57	126	9.91	1.23	11.8
PGC50404	14 07 42.2	-38 09 58	62	1.61	0.17	15.8
PGC50942	14 15 34.3	+36 13 36	112	6.38	0.69	13.1
PGC52809	14 47 24.2	-17 26 44	171	3.70	0.50	14.0
PGC54392	15 14 13.6	-46 48 36	36	10.86	1.05	11.9
PGC57349	16 10 04.8	+22 39 00	14	1.65	0.21	15.5
PGC57582	16 14 25.0	-00 12 26	90	5.71	0.58	13.5
PGC59635	17 07 00.1	-62 04 59	136	4.98	0.44	13.9

Name	RA(2000)	Dec(2000)	PA (Deg)	MajA (arcmin)	MinA	Btot mag
PGC61300	18 01 51.6	+06 58 11	3	5.38	0.68	13.4
PGC62198	18 39 02.5	-55 37 03	141	1.45	0.17	15.7
PGC63317	19 31 16.8	+42 11 56	89	1.43	0.17	15.8
FGC1418	19 59 15.7	-20 47 47	50	0.56	0.05	18.0
PGC64133	20 07 14.5	-69 28 44	28	1.27	0.17	15.6
PGC68327	22 13 38.9	+14 13 09	144	2.24	0.28	15.4
PGC68389	22 14 55.3	-66 50 56	29	4.89	0.61	13.5
PGC70708	23 13 13.2	+06 25 48	145	4.70	0.45	14.0

Transiting Extra-Solar Planets

This project aims to observe a transit of an extra-solar planet (exoplanet). Exoplanets are planets orbiting stars other than our own sun. If an exoplanet crosses in front of its parent star from our point of view, it will block a small portion of the star's light causing the star to dim slightly. We can measure this drop in brightness, and determine the exoplanet's radius and (from repeated transit observations) its orbital period.

The transit method has been one of the most powerful tools for detecting new exoplanets. As of October 2020, 3261 exoplanets have been discovered using the transit method (c.f. 820 from radial velocity).



An example of a lightcurve for a transiting planet. (Credit: NASA Ames)

Listed below are a number of stars hosting transiting exoplanets. Some of these stars will be observable during the workshop. Keep in mind that transits are time specific. While the host star may be observable during a night, the exoplanet may not be transiting at that time. In addition to determining if the star is observable, you will have to check if the exoplanet is transiting during your observing period. A tool that may be useful for this is the Exoplanet Transit Database (http://var2.astro.cz/ETD/index.php)

A selection of stars hosting transiting exoplanets

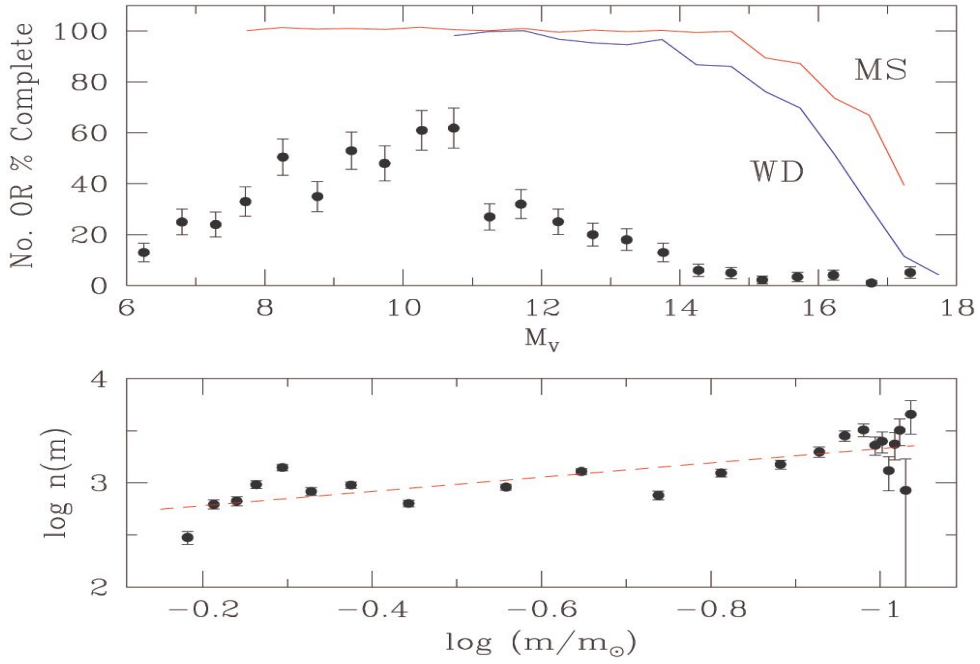
Object	RA (J2000)	Dec (J2000)	V Mag	Transit Depth (Mag)
Qatar-5	00 28 12.94	+42 03 40.9	12.62	0.0119
WASP-33	02 26 51.08	+37 33 02.5	8.3	0.0151
WASP-12	06 30 32.79	+29 40 20.4	11.69	0.0151
OGLE-TR-113	10 52 24	-61 26 48	14.42	0.0245
HAT-P-36	12 33 03.96	+44 54 55.30	12.26	0.02044
HAT-P-44	14 12 34	+47 00 52.9	13.21	0.0194
TOI-3984 A	15 05 20.92	+36 47 13.11	15.694	0.0234
WASP-135	17 49 08.3939	+29 52 44.741	13.28	0.0226
HAT-P-63	17 58 17.31	+05 45 40.9	13.7	0.01458
HAT-P-5	18 17 37.30	+36 37 16.6	12.0	0.0142
CoRoT-11	18 42 44.95	05 56 16.12	12.94	0.0123
TrES-2	19 07 14	+49 18 59	11.41	0.0169
Kepler-45	19 31 29	+41 03 51	16.74	0.03284
WTS-1	19 35 58.37	+36 17 25.17	16.644	0.0190
Kepler-15	19 44 48	49 08 24	13.758	0.0114
Kepler-17	19 53 34.86	+47 48 54.0	14.14	0.0213
HD189733	20 00 43.713	+22 42 39.07	7.67	0.0282
TrES-5	20 20 53	+59 26 55	13.7	0.0215
WASP-46	21 14 56.86	-55 52 18.1	12.9	0.0204
HAT-P-1	22 57 47	+38 40 30	10.4	0.0171
WASP-4	23 34 15.06	-42 03 41.1	12.5	0.0194
WASP-5	23 57 23.74	-41 16 37.5	12.3	0.0137

Globular Clusters

Globular cluster stars are distinctly different than most stars. They are some of the oldest objects in the galaxy and their formation remains poorly understood. They have different spatial distribution and chemical composition than that of non-clustered stars. These differences reveal a different aspect of galactic structure than ordinary stars. In part because of these differences, globular clusters inform us of the formation and early evolution of galaxies.

Some ongoing projects include determining the main sequence (MS) luminosity function (LF) to very faint limits, globular cluster formation and dynamical evolution, and detecting and measuring variable stars (such as Cepheid and RR Lyrae stars) and using their period–luminosity relationship for making distance estimates.

The goal of this project is to select a few globular clusters and collect enough data to determine the population distribution of MS stars as a function of magnitude. Then compare the globular cluster to each other and M4 (as shown below).



Top panel: M4 MS LF corrected for completeness for both MS and white dwarf (WD) stars. Bottom panel: M4 MS Mass Function (MF) with power-law slope alpha = 0.75 indicated. - Richer et. al APJ 574:L151–L154, 2002 August 1

Target List

Object	Alt Name	RA (J200)	DEC (J2000)	Mag (V)
NGC 104	47 Tuc	00 24 05.2	-72 04 51	4.91
NGC 288		00 52 47.5	-26 35 24	9.37
NGC 362		01 03 14.3	-70 50 54	7.21
Pal 1		03 33 23.0	+79 34 50	13.2
AM 1		03 55 02.7	-49 36 52	15.7

Eridanus		04 24 44.5	-21 11 13	14.7
Pal 2		04 46 05.9	+31 22 51	13.0
NGC 1851		05 14 06.3	-40 02 50	8.05
NGC 1904	M 79	05 24 10.6	-24 31 27	8.56
NGC 2419		07 38 08.5	+38 52 55	10.4
AM 2		07 39 11.1	-33 50 57	?
NGC 2808		09 12 02.6	-64 51 47	6.89
Pal 3		10 05 31.4	+00 04 17	13.9
NGC 3201		10 17 36.8	-46 24 40	8.24
Pal 4		11 29 16.8	+28 58 25	14.2
Rup 106		12 38 40.2	-51 09 01	10.9
NGC 4590	M 68	12 39 28.0	-26 44 34	9.67
NGC 4833		12 59 35.0	-70 52 29	7.79
NGC 5024	M 53	13 12 55.3	+18 10 09	8.33
NGC 5694		14 39 36.5	-26 32 18	10.89
NGC 5904	M 5	15 18 33.8	+02 04 58	6.65
NGC 5927		15 28 00.5	-50 40 22	8.86
NGC 6093	M 80	16 17 02.5	-22 58 30	7.87
NGC 6121	M 4	16 23 35.5	-26 31 31	7.12
Terzan 3		16 28 40.1	-35 21 13	12
NGC 6341	M 92	17 17 07.3	+43 08 11	6.3
NGC 6333	M 9	17 19 11.8	-18 30 59	8.42
Terzan 2		17 27 33.4	-30 48 08	14.3
NGC 6528		18 04 49.6	-30 03 21	10.65
Djorg 3		18 06 08.6	-27 45 55	9.3
NGC 6541		18 08 02.2	-43 42 20	7.32
NGC 6553		18 09 15.6	-25 54 28	8.1
IC 1276	Pal 7	18 10 44.2	-07 12 27	10.3
Terzan 12		18 12 15.8	-22 44 31	15.6
NGC 6779		19 16 35.5	+30 11 05	8.3
Pal 10		19 18 02.1	+18 34 18	13.2
NGC 6838	M 71	19 53 46.1	+18 46 42	6.1
NGC 6864	M 75	20 06 04.8	-21 55 17	9.18
NGC 7078	M 15	21 29 58.3	+12 10 01	6.2
NGC 7089	M 2	21 33 29.3	-00 49 23	6.3
Pal 13		23 06 44.4	+12 46 19	13.5

Planetary Nebulae Expansion Velocities

Planetary nebulae (PNe) are the glowing shells of gas and plasma ejected by stars less than about 8 solar masses when they die. During the red giant phase the outer layers of the star are expelled via pulsations and strong stellar winds.

Expansion velocities for PNe are measured by calculating the width of the emission lines, typically HI, HeII, [NII] and [OIII]. Expansion velocities can be used to examine the dynamical processes along the minor and major axes to better understand the morphology and evolution of PNe. Typical expansion velocities are on the order of 10 - 100 km/s.

One can also use these same data to calculate emission line ratios, which can illuminate the kinematics of the ionized gas.

V_{Int} is the integrated magnitude of the nebula, while V_{WD} is the magnitude of the central white dwarf.

Potential Targets:

Abell	RA(2000)	Dec(2000)	V_{Int}	V_{WD}	Diameter(arcmin)
01	00 12 54.6	+69 10 23	18.0	20.5	0.8
05	02 52 14.8	+50 35 54	16.0	21.4	2.1
08	05 06 38.4	+39 08 09	16.6	20.2	1.0
13	06 04 47.8	+03 56 36	15.3	19.8	2.9
16	06 43 54.9	+61 47 25	14.5	17.4	2.3
21	07 29 04.5	+13 14 55	10.3	15.9	10.3
25	08 06 46.0	-02 52 42	15.4	18.9	2.8
29	08 40 17.0	-20 54 14	14.3	18.3	6.7
33	09 39 09.1	-02 48 32	12.6	15.5	4.5
36	13 40 41.3	-19 52 57	11.8	11.5	6.2
41	17 29 02.2	-15 13 07	17.2	16.5	0.3
45	18 30 16.1	-11 36 56	12.8	21.1	4.8
49	18 53 28.6	-06 28 35	16.1	21.0	0.6
53	19 06 46.1	+06 23 50	15.5	20.9	0.5
57	19 17 05.9	+25 37 33	14.7	17.6	0.6
61	19 19 10.3	+46 14 51	13.5	17.3	3.3
65	19 46 34.3	-23 08 14	13.2	15.9	2.1
69	20 19 58.4	+38 23 59	18.7	21.0	0.4
73	20 56 26.7	+57 26 00	16.5	21.1	1.2
77	21 32 10.3	+55 52 42	15.0	15.7	1.3
81	22 42 25.3	+80 26 28	14.0	18.8	0.6
86	00 01 30.9	+70 42 30	16.7	20.0	1.1

Quasar Redshifts

Quasars are supermassive blackholes at the centers of galaxies actively accreting material. The emission of the accretion disks excites gases causing broad and/or narrow-line emission.

Quasars usually have distinctive emission lines from, for example, hydrogen, oxygen, nitrogen, and magnesium that can be used to measure their redshift, z, (i.e., $\lambda=(1+z)\lambda_o$) and, consequently, their distance based on Hubble's Law, $v=H_0 * D$. Typical emission lines are H-alpha at 6563Å, H-beta at 4861Å, and [OIII] at 5007Å. Measuring the redshifts, and hence distances, to quasars (and their host galaxies), enables one to understand the structure of the universe and the evolution of quasars.

Potential Targets:

Name	RA(2000)	Dec(2000)	V
B0026+129	00 29 13.73	+13 16 04.4	15.41
J0047+0319	00 47 05.70	+03 19 57.3	16.00
LBQS0046-2914	00 49 16.71	-28 58 19.5	18.00
B0318-1937	03 20 21.14	-19 26 31.0	14.86
J0407-1211	04 07 48.41	-12 11 35.9	15.35
B0731+479	07 35 02.22	+47 50 07.7	18.00
B0814+350	08 17 40.16	+34 54 52.3	20.00
3C 206	08 39 50.61	-12 14 33.9	15.76
J0854+1930	08 54 50.68	+19 30 37.4	18.00
B0907-091	09 09 36.17	-09 18 19.2	18.00
7C 1011+2503	10 13 53.44	+24 49 17.1	15.40
B1015+383	10 18 25.01	+38 05 22.6	18.00
B1022-099	10 24 48.12	-10 09 33.8	18.00
4C 16.30	11 07 15.07	+16 28 02.7	15.70
B1138+5826	11 41 21.68	+58 09 51.9	18.00
B1151+117	11 53 49.90	+11 28 28.4	15.51
B1200-051	12 02 34.42	-05 28 06.3	18.00
B1217+023	12 20 11.90	+02 03 42.1	15.93
LBQS1228+1116	12 30 54.06	+11 00 10.2	18.00
LBQS1234-0212	12 36 39.85	-02 28 37.0	18.00
J124808.4-004324	12 48 08.40	-00 43 23.4	18.00
B1249+272	12 51 50.28	+26 56 37.3	20.00
B1252+0200	12 55 19.65	+01 44 12.5	15.48
B1310-1332	13 13 06.55	-13 48 31.0	20.00
B1322+6557	13 23 49.54	+65 41 48.0	15.86
J134350.6+264930	13 43 50.55	+26 49 29.8	20.00
B1347.3+2707	13 49 38.15	+26 52 39.1	20.00
B1348+384	13 50 15.15	+38 12 06.6	18.00
B1414-2510	14 16 55.82	-25 24 12.7	15.50

Name	RA(2000)	Dec(2000)	V
J1446+4035	14 46 45.94	+40 35 06.0	15.95
B1449+588	14 50 26.72	+58 39 44.7	16.00
3C 311	15 04 09.14	+60 00 56.1	18.00
4C 37.43	15 14 43.06	+36 50 50.5	15.50
B1617+1731	16 20 11.66	+17 24 26.8	15.46
B1623+271	16 25 09.41	+27 02 55.9	18.00
B1640+3944	16 42 11.17	+39 38 35.9	18.00
B1652+151	16 54 51.71	+15 02 56.3	18.00
J1701+5149	17 01 24.93	+51 49 21.2	15.43
B2127+176	21 29 38.30	+17 54 47.0	18.00
B2203-202	22 06 25.02	-19 57 39.9	20.00
B2229-4211	22 32 50.66	-41 56 19.8	20.00
B2258-391	23 01 30.47	-38 54 03.6	18.00
B2303+183	23 06 22.09	+18 40 00.8	18.00
B2302-783	23 06 50.67	-78 07 52.2	15.44
B2355-364	23 57 39.54	-36 08 29.6	18.00

Seyfert Galaxy Classification

Seyfert galaxies are characterized by the presence of strong, high-ionization emission lines such as [OIII] 4363, 4959, and 5007. Khachikian and Weedman (1974) identified two subclasses of Seyfert galaxies, as determined by the presence or absence of broad bases on the permitted emission lines in their spectra. Seyfert 2 galaxies show only one set of emission lines which are comparatively narrow and originate from low-density ionized gas (electron density 10^3 to 10^6 electrons/cm^3) with widths corresponding to several 100 km/s as indicated from the line width, which is somewhat broader than the emission lines from non-active galactic nuclei. These lines are frequently referred to as "narrow lines" and occur for both permitted and forbidden spectral lines. Seyfert 1 galaxies, in addition, show a set of "broad lines" corresponding to velocities up to 1000 km/s, occurring only for the permitted lines, which indicates higher densities (10^9 electrons/cm^3).

Osterbrock (1981) introduced subclasses of Seyfert 1 galaxies based on spectroscopic details: 1.5, 1.8, and 1.9. For 1.9, the broad lines are only detectable for H alpha lines, while for 1.8, weak broad H beta lines can be detected also, and for Seyfert 1.5 nuclei, the strengths of broad and narrow H beta components are comparable.

Aretxaga, et al (1999) show that Seyferts can change over time from one classification to another, in this case NGC 7582 transitioned from a classical type 2 Seyfert towards a type 1. Causes of these changes in type could be due one of the following: capture of a star by a supermassive black hole, reddening change in the surrounding torus, or the radiative onset of a Type IIn supernova exploding in a compact nuclear/circumstellar starburst.

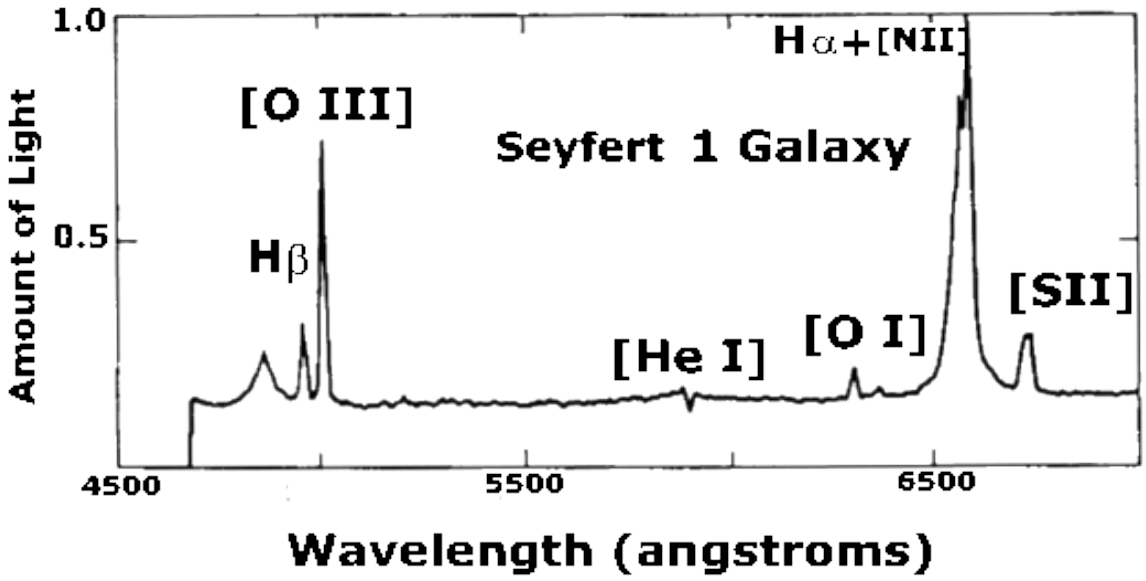
We aim to monitor Seyfert Galaxies and classify them to identify changes in their spectra and evaluate possible causes for the transition.

Potential Targets:

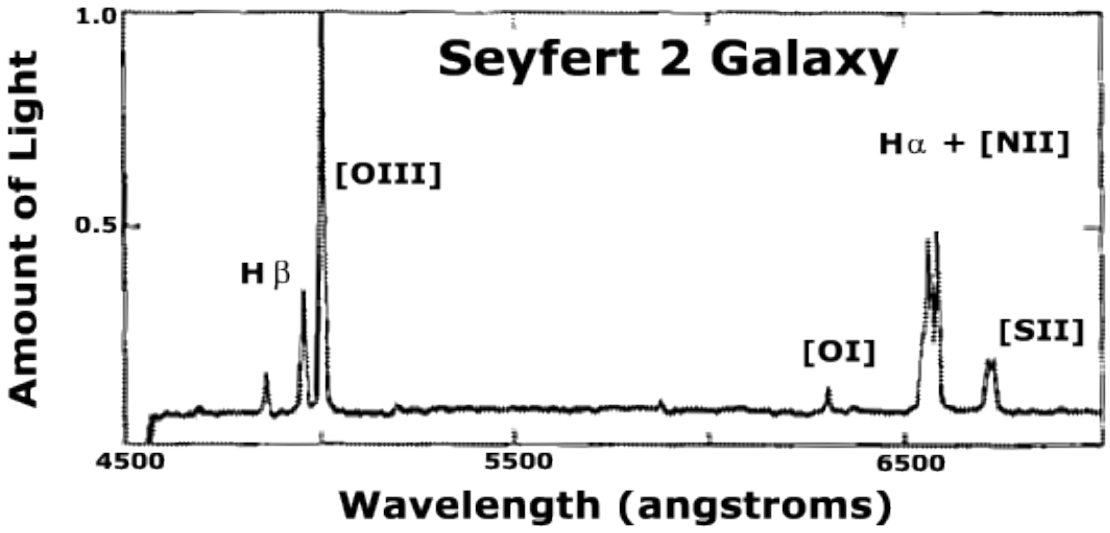
Name	**RA(2000)**	**Dec(2000)**	**B**
IAU0000+044	00 03 09.8	+04 45 42	17.00
Mrk335	00 06 19.5	+20 12 11	14.2
IAU0008-213	00 10 54.7	-21 04 06	15.00
IAU0102-643	01 04 27.9	-64 07 20	14.88
Mrk1155	01 26 12.5	+33 24 18	15.0
NGC566	01 29 03.1	+32 19 56	14.6
IAU0158+263	02 01 44.4	+26 32 27	14.40
NGC985	02 34 37.8	-08 47 15	14.5
NGC1068	02 42 40.8	-00 00 48	9.7
NGC1275	03 19 48.2	+41 30 42	13.1
IAU0351+026	03 54 10.0	+02 49 21	17.30
NGC1566	04 20 00.6	-54 56 17	10.2
IAU0549-074	05 52 11.4	-07 27 23	13.77
Mrk3	06 15 36.3	+71 02 15	13.8

Name	RA(2000)	Dec(2000)	B
IAU0651+542	06 55 14.8	+54 08 57	19.51
IAU0831+557	08 34 54.9	+55 34 21	19.00
IAU0835+250	08 38 11.0	+24 53 44	14.72
IAU0957-225	09 59 29.8	-22 49 35	12.70
NGC3227	10 23 30.6	+19 51 54	12.2
IAU1058+113	11 01 01.8	+11 02 48	16.48
NGC3516	11 06 47.6	+72 34 08	12.3
IAU1116-291	11 18 53.9	-29 25 31	15.00
NGC4051	12 03 09.6	+44 31 53	11.5
NGC4151	12 10 32.7	+39 24 20	11.2
NGC4258	12 18 57.5	+47 18 14	9.6
IAU1258-306	13 01 20.1	-30 56 08	15.00
IAU1331-234	13 34 36.5	-23 40 47	15.00
IAU1351+640	13 53 15.8	+63 45 44	15.01
IAU1351+236	13 54 06.3	+23 25 46	15.87
NGC5548	14 18 00.0	+25 08 13	13.1
IAU1530-085	15 33 18.9	-08 41 25	16.80
IAU1641+398	16 43 22.2	+39 48 24	15.00
IAU1729+596	17 30 22.3	+59 38 22	15.40
IAU1833+326	18 35 03.4	+32 41 47	15.56
NGC6814	19 42 40.4	-10 19 24	11.9
IAU2014-558	20 18 01.2	-55 39 31	15.50
Mrk509	20 44 09.8	-10 43 25	13.0
IAU2121+248	21 23 44.6	+25 04 28	17.33
IAU2121-179	21 24 41.4	-17 44 46	16.50
IAU2125-149	21 28 39.0	-14 43 32	19.52
IAU2130+099	21 32 27.7	+10 08 19	14.63
IAU2204-409	22 07 04.6	-40 44 37	20.90
IAU2224-354	22 27 10.7	-35 08 41	16.00
NGC7469	23 03 15.8	+08 52 26	13.0
NGC7742	23 44 15.9	+10 46 01	12.5
IAU2353-012	23 56 09.8	-00 59 18	14.80

Seyfert 1 spectrum



Seyfert 2 spectrum



Light Curves of Supernovae

Studies of nearby supernovae (SNe) are critical to furthering our understanding of a star in its final death throes. Filtered light curves of a SN give insight into the physical mechanisms powering the explosion.

Professor Alex Filippenko's research group at UC Berkeley is involved in a large, long-term campaign to amass a database of BVRI photometry for the various types of SNe (e.g., Type Ia, Ib, II-P, II-L; see Figure 1). Non-robotic telescopes are used by their group to acquire late-time photometry of SNe to be used in addition with nightly data acquired with the robotic telescope KAIT.

The goal is to observe as many SN fields as the night allows, obtaining images through each of the B, V, R, and I filters. On photometric (cloudless) nights, Landolt standard stars are observed at a variety of airmasses. This allows one to derive a photometric solution, which can then be used to transform instrumental magnitudes into standard magnitudes.

A signal from the SN of a few hundred (~500) counts above background is sufficient for these data. The average magnitude of the SNe's host galaxies is about 15, while the standards are about 11.

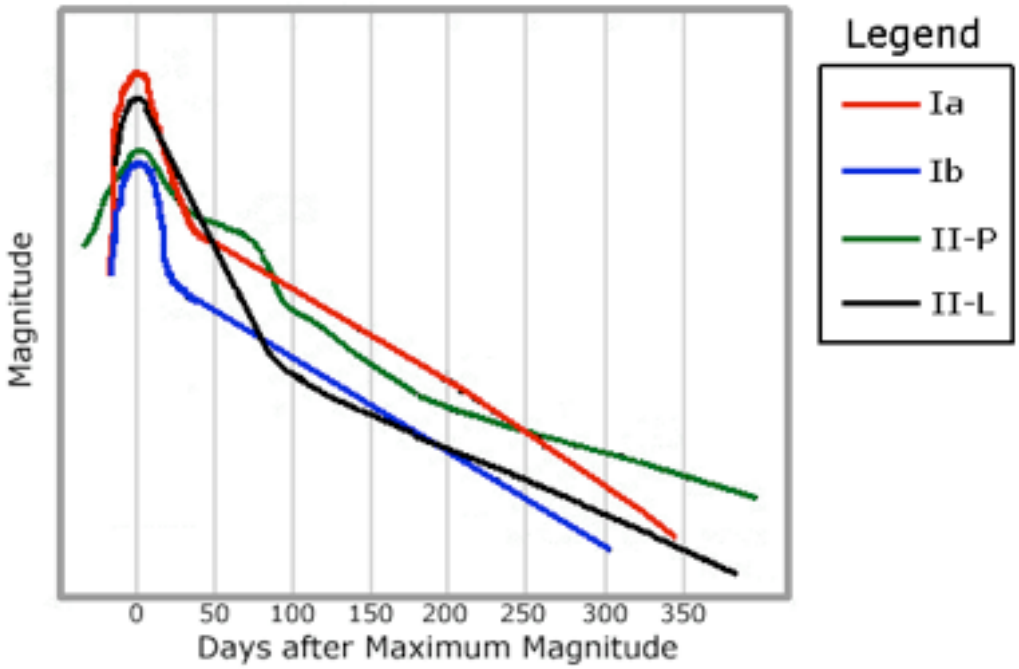


Figure 1. A plot showing light curves (change in brightness over time) for four types of supernovae.

Potential Targets

Name	Date First Observed	RA (J2000)	Dec (J2000)	Latest Mag	Date Last Observed
2026sqf	2026/07/08	10:38:47.961	+53:30:34.10	12.5	2026/10/01
2026aaiv	2026/09/01	22:37:05.618	+34:24:35.37	13.0	2026/10/01
2026acxa	2026/09/25	21:02:30.263	-19:27:41.91	14.9	2026/09/30
2026abxl	2026/09/16	13:23:45.388	+31:33:52.17	15.5	2026/09/16
2026pub	2026/06/21	13:45:37.479	-05:59:35.83	16.0	2026/08/05
2026zji	2026/08/21	20:04:34.466	+62:38:38.73	16.2	2026/09/23
2026abpr	2026/09/11	23:45:33.379	-24:12:30.90	16.2	2026/09/16
2026yly	2026/08/09	09:13:38.170	+76:28:18.10	16.3	2026/09/28
2026yid	2026/08/07	20:22:32.434	-50:45:14.36	16.3	2026/09/26
2026acjs	2026/09/20	18:54:32.345	-62:51:31.44	16.4	2026/09/25
2026plb	2026/05/21	20:56:47.260	-18:31:04.49	16.8	2026/09/20
2026fov	2026/03/14	22:28:27.241	+30:17:54.46	16.8	2026/09/23
2026zoa	2026/08/23	02:16:27.519	-59:56:34.64	16.9	2026/09/16
2026ziq	2026/08/20	21:22:31.171	-36:40:53.45	16.9	2026/08/20
2026yzg	2026/08/15	13:30:59.077	-27:02:34.59	16.9	2026/08/15
2026weo	2026/07/24	01:10:22.021	-09:34:08.15	16.9	2026/09/10
2026mho	2026/05/12	20:07:38.301	-21:07:06.40	16.9	2026/08/19

(http://www.rochesterastronomy.org/snimages/snactive.html)

Name	RA(J2000)	Dec(J2000)	
92_507	00 56 51	+01 07 46	standard
93_317	01 54 38	+00 43 00	standard
PG0231+051	02 33 41	+05 18 40	standard
95_96	03 53 01	+00 00 13	standard
96_36	04 51 43	-00 10 12	standard
98_650	06 52 12	-00 19 17	standard
ru152	07 29 56	-02 05 39	standard
m67	08 51 18	+11 45 46	standard
PG0918+029	09 21 35	+02 46 20	standard
PG1047+003	10 50 10	-00 01 08	standard
104_461	12 43 11	-00 32 51	standard
PG1323-086	13 25 44	-08 50 22	standard
hd121968	13 58 52	-02 55 12	standard
107_458	15 38 51	-00 23 30	standard
PG1633+099	16 35 32	+09 46 43	standard
109_954	17 44 15	-00 02 17	standard
110_499	18 43 13	+00 29 00	standard
111_773	19 37 16	+00 11 30	standard
112_250	20 42 31	+00 07 30	standard
113_339	21 40 56	+00 27 57	standard
114_654	22 41 30	+01 10 41	standard
PG2336+004	23 38 41	+00 42 30	standard

Symbiotic Stars

Symbiotic stars are binary systems consisting of a cool giant star and a small hot star such as a white dwarf. Their optical spectra display a combination of a late M type stellar spectrum with molecular absorption bands from species like TiO and emission lines from high excitation species such as HeII and [OIII]. The emission arises from the stars themselves and the nebulosity that surrounds them. About half of the symbiotic stars display broad highly polarized emission lines at λ6830 and λ7088 that remained a mystery for over fifty years until 1989 when H. M. Schmid (A&A, 211, L31) proposed that they were due to Raman scattering of OVI λ1032 and λ1038 photons coming from the white dwarf by neutral hydrogen in the atmosphere and wind of the red giant. Because the scattering geometry is anisotropic with the incident photons arising from the white dwarf and the scattered photons arising from the atmosphere of the red giant the scattered lines can exhibit a high degree of polarization. In addition, since the scattering geometry varies in a systematic way in a binary system, the observed polarization in the scattered lines will also vary systematically. Modeling the temporal variation in the polarization of the Raman scattered lines serves as a diagnostic for the orbital elements of the binary system.

The goal of this project is to obtain a time series of spectropolarimetric observation of a group of symbiotic stars in order to monitor the polarization in the Raman scattered emission lines as a function of time with the aim of determining the orbital elements of these binary stars. Typical orbital periods are in the range of several hundred days.

Targets:

Name	**RA(J2000)**	**Dec(J2000)**	**B**	**J**
SY Mus	11 32 10.0	-65 25 11	11.3	5.9
AG Dra	16 01 41.0	+66 48 10	11.3	7.2
RT Ser	17 39 52.0	-11 56 39	10.6	8.4
HM Sge	19 41 57.1	+16 44 40	11.1	7.6
CI Cyg	19 50 11.8	+35 41 03	11.9	5.8
V1016 Cyg	19 57 05.0	+39 49 36	10.0	7.0
RR Tel	20 04 18.5	-55 43 33	6.5	7.3
CD-43°14304	21 00 06.4	-65 25 11	12.6	8.6
Z And	23 33 40.0	+48 49 06	11.9	6.2

Unpolarized Standard Stars

Name	**RA(B1950)**	**Dec(B1950)**	**V**
HD 432	00 06 29.7	+58 52 27	2.4
HD 185395	19 35 06.0	+50 06 16	4.5

Polarized Standard Stars

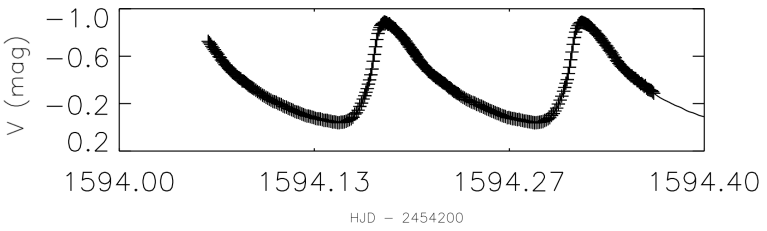
Name	**RA(B1950)**	**Dec(B1950)**	**V**
HD 7927	01 16 55.1	+57 58 10	5.0
HD 183143	19 25 13.2	+18 11 37	6.9

Variable Stars

δ-Scuti stars are a type of variable star in which the star pulsates, expanding and contracting in a cyclic manner leading to variations in luminosity. There is a relationship between the period over which the δ-Scuti star varies and its intrinsic luminosity, which allows us to use δ-Scuti stars as 'standard candles' to determine distances to e.g. star clusters or nearby galaxies.

A sub-class of δ-Scuti stars are SX Phoenicis (SX Phe) stars. SX Phe stars are generally older stars with low metallicity, and are commonly found in Globular Clusters. SX Phe stars exhibit larger variations in luminosity than other δ-Scuti stars, over periods typically $\sim$1-2 hours.

Our goal here is to observe SX Phe stars over the course of an observing session and monitor the brightness to construct a lightcurve.



Lightcurve of XX-Cygni from Yang et al. 2012 (AJ, 144, 92)

A selection of SX Phe stars

Object	RA (J2000)	Dec (J2000)	V Mag	Period (Hours)
GD 428	03 47 19.88	+63 22 42.1	12.93	0.94
AE UMa	09 36 53.16	+44 04 00.4	11.35	2.06
KZ Hya	10 50 54.07	-25 21 14.7	10.06	1.44
V459 Vir	13 13 22.73	-02 05 28.89	13.91	4.49
LZ Her	17 49 29.20	+29 19 15.74	13.48	3.05
LW Dra	19 06 26.32	+68 29 01.59	10.82	2.84
XX Cygni	20 03 15.64	+58 57 16.5	11.86	3.24
CY Aquarii	22 37 47.85	+01 32 03.8	10.44	1.46
DY Pegasi	23 08 51.19	+17 12 56.0	10.26	1.75
BX Scl	23 43 54.46	-28 18 34.6	13.56	0.89
SX Phoenicis	23 46 32.89	-41 34 54.8	7.12	1.32

Spectroscopic Binaries

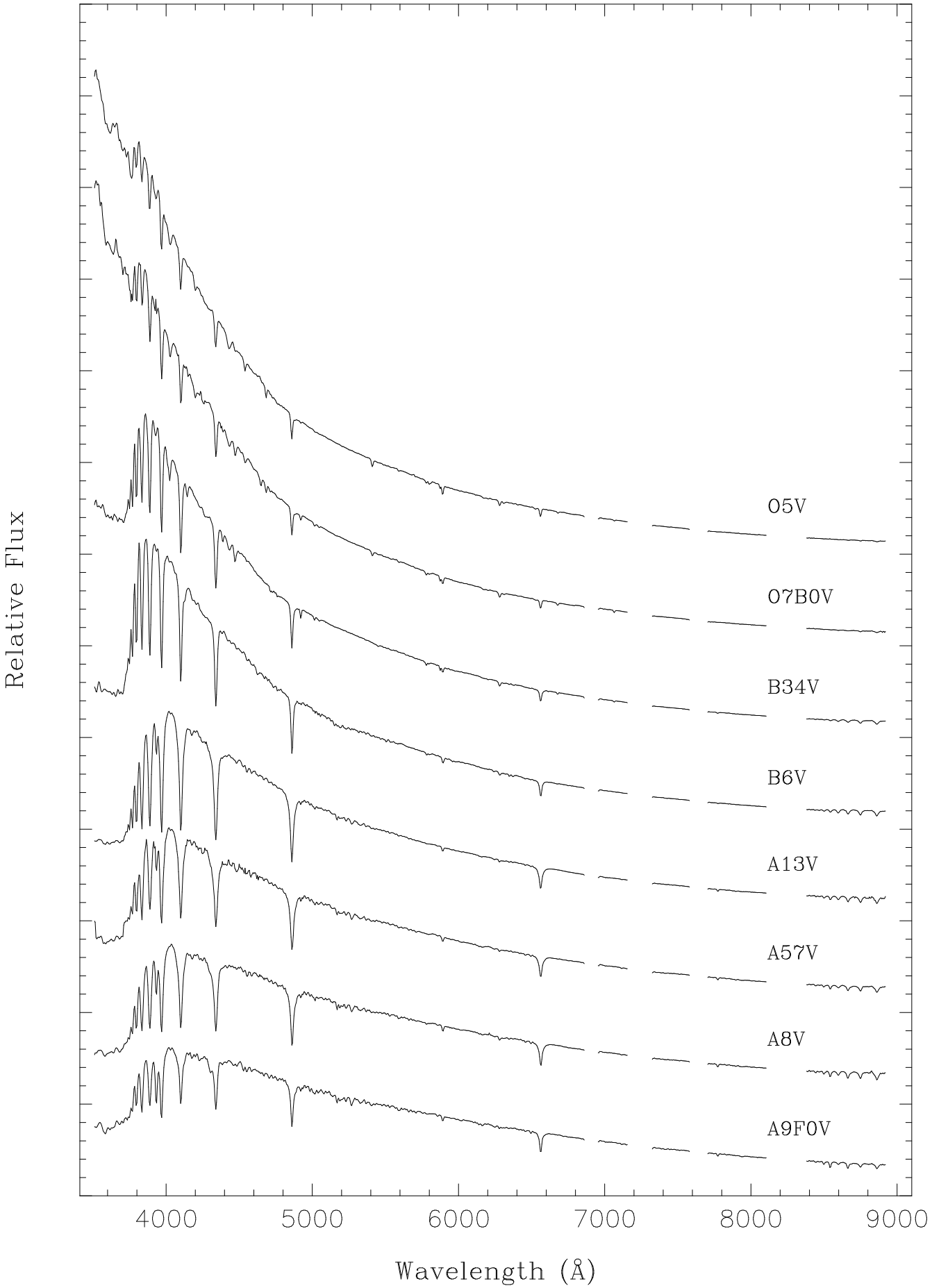
Roughly 33% of stars are binary (or multiple) stellar systems (Lada, 2006), with early type stars more likely to be in binary or multiple systems than low mass stars. While some binary stars are easily identified visually, a vast number are only identifiable from their spectra.

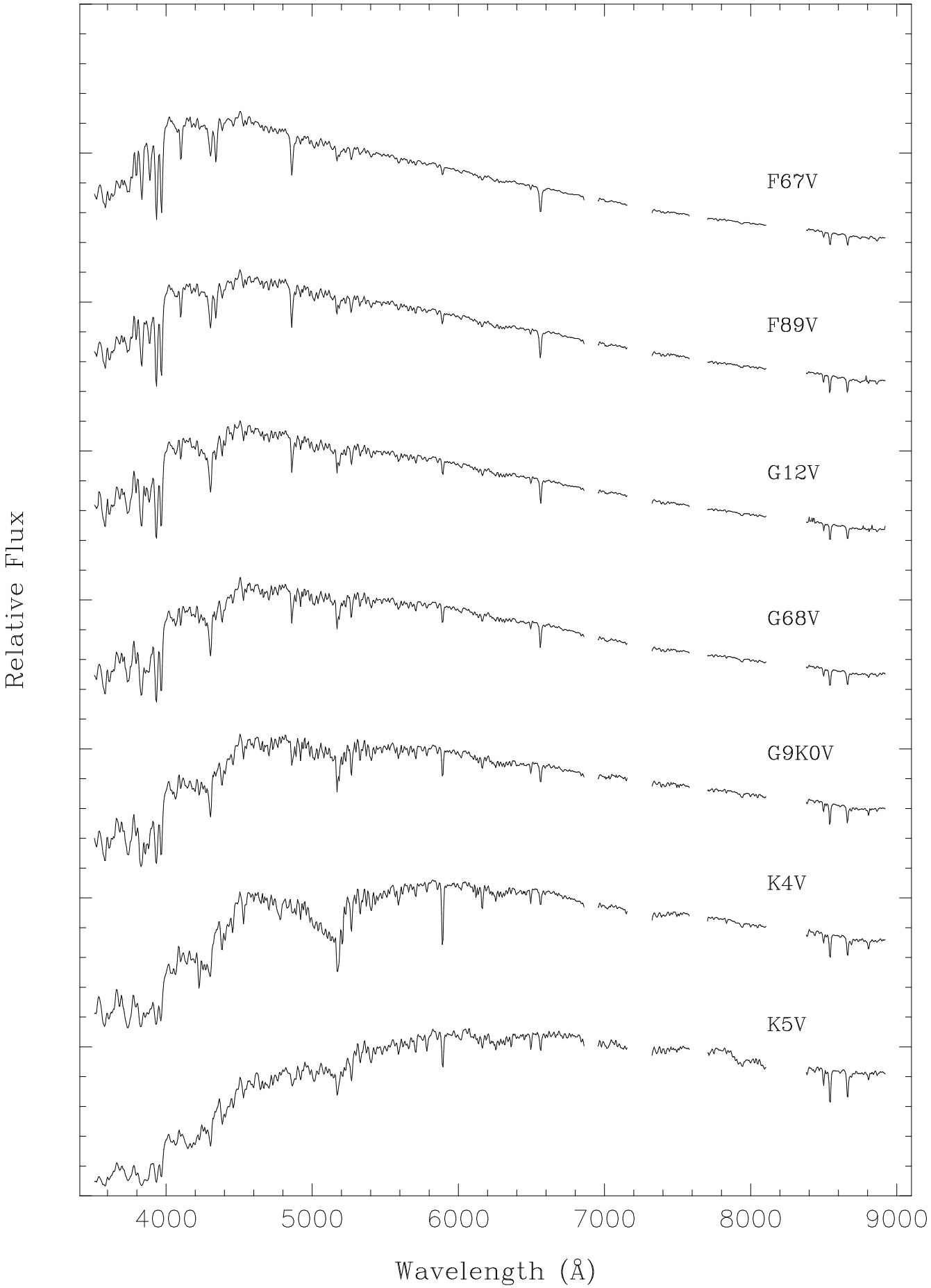
Identification of both spectral type and radial velocities from the spectra give us valuable insight into the physical parameters of the system, such as temperatures and masses of the component stars in addition to the orbital parameters. We aim to identify the spectral types of the component stars.

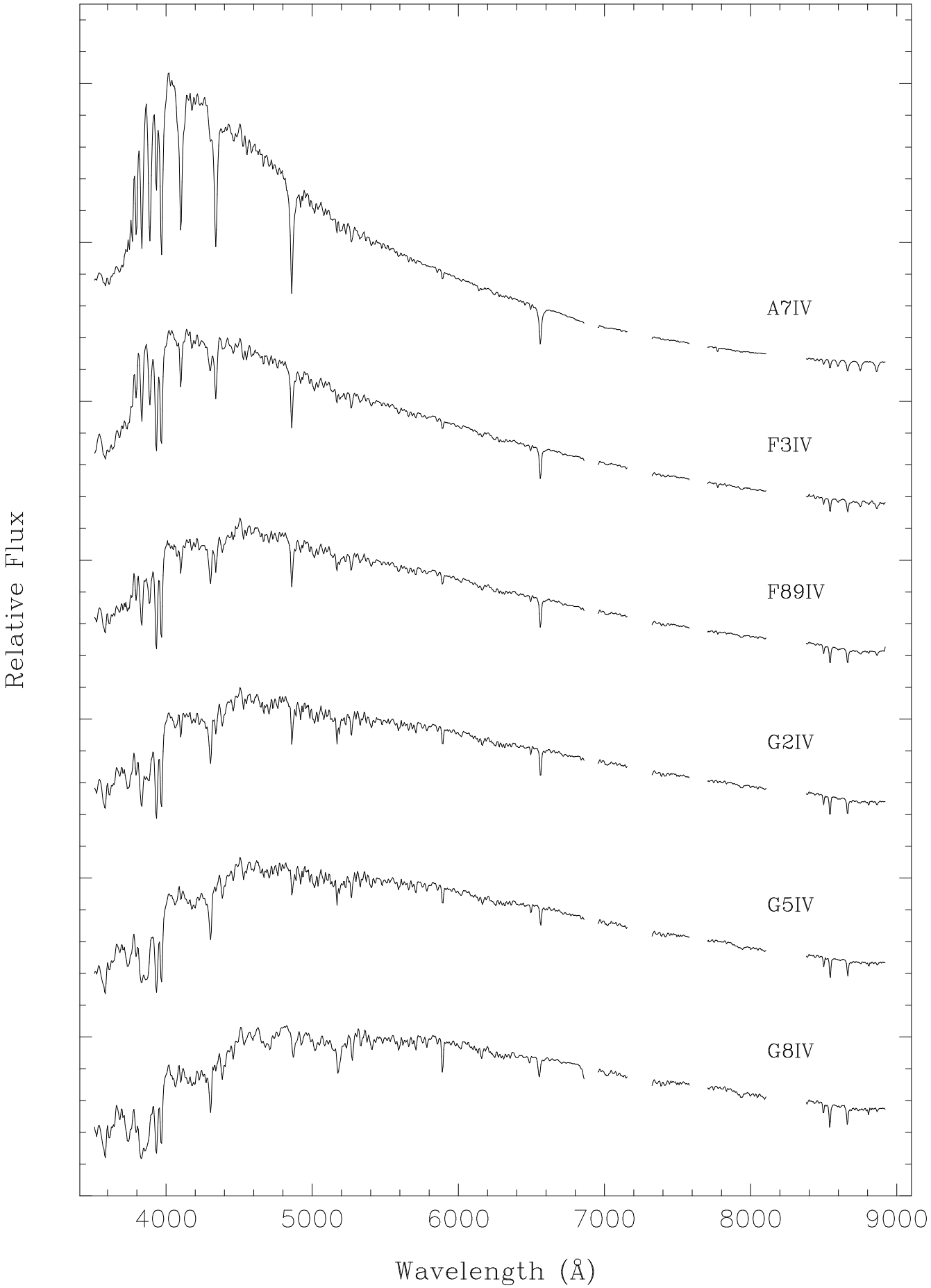
Potential Targets:

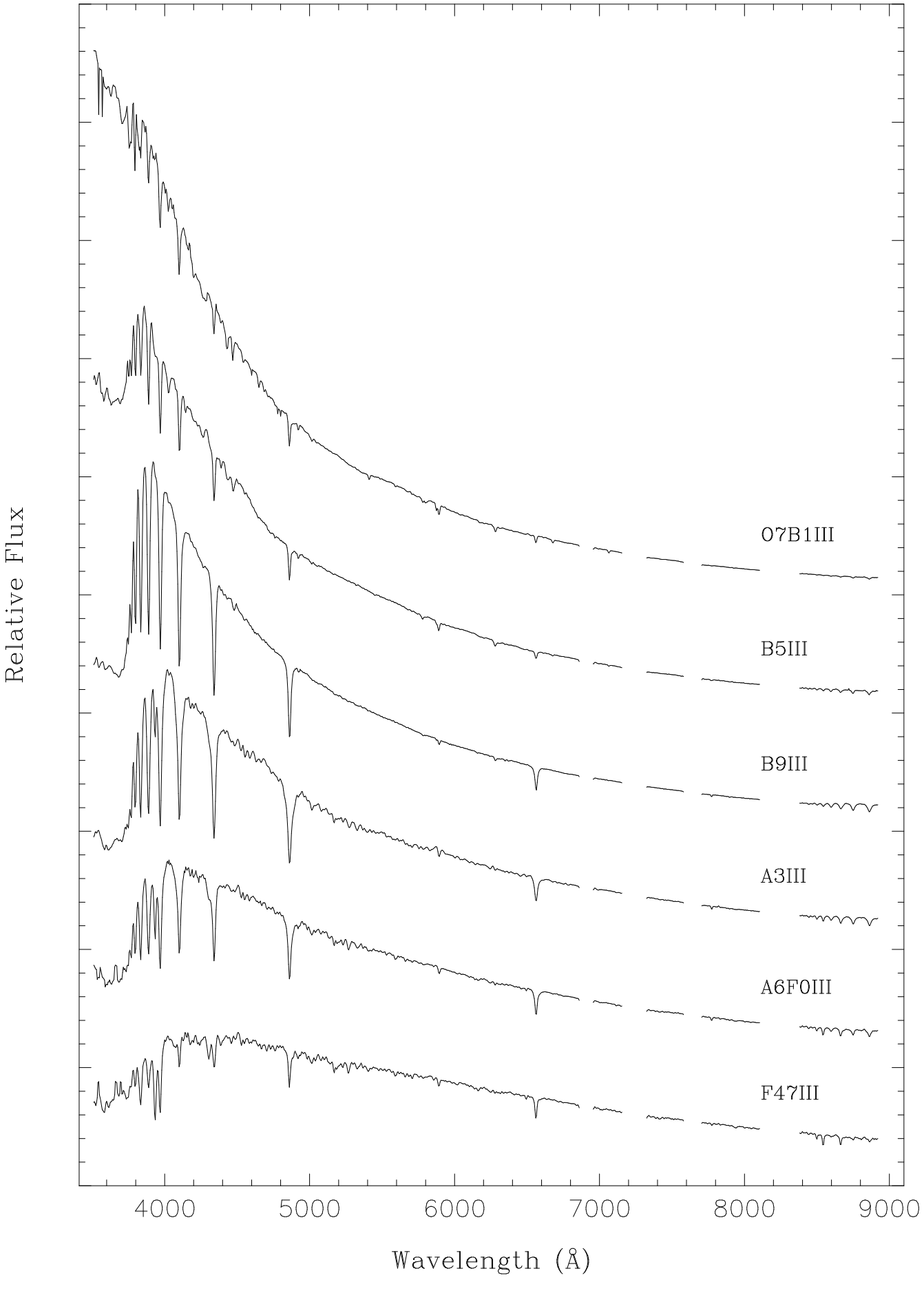
Object	RA(2000)	Dec(2000)	V
SX Cas	00 10 42.1	+54 53 29	9.05
UU Psc	00 14 58.8	+08 49 15	6.01
AQ Cas	01 19 10.3	+62 23 48	10.3
IZ Per	01 32 05.5	+54 01 08	7.95
AE Phe	01 32 32.9	-49 31 41	7.79
DM Per	02 25 58.007	+56 06 10.01	7.95
CC Eri	02 34 22.566	-43 47 46.87	8.70
UX Ari	03 26 35.389	+28 42 54.32	6.47
GK Per	03 31 11.82	+43 54 16.8	12.88
YY Eri	04 12 08.850	-10 28 09.96	8.41
51 Tau	04 18 23.202	+21 34 45.47	5.64
IM Aur	05 15 29.746	+46 24 21.46	8.11
EW Ori	05 20 09.147	+02 02 39.97	9.83
SV Cam	06 41 19.074	+82 16 02.42	9.37
RW Mon	06 34 45.890	+08 49 32.18	9.32
Y Cam	07 41 11.008	+76 04 26.12	10.56
KQ Pup	07 33 47.95	-14 31 26.2	4.97
SW Lyn	08 07 41.571	+41 48 01.71	9.66
HD 67198	08 03 29.708	-60 31 31.13	9.04
HD 81410	09 24 49.015	-23 49 34.71	7.37
W UMa	09 43 45.469	+55 57 09.07	7.96
HS Hya	10 24 36.768	-19 05 32.96	8.12
YZ Car	10 28 16.847	-59 21 00.68	8.69
TT Hya	11 13 12.497	-26 27 54.25	7.31
RW UMa	11 40 46.352	+51 59 53.41	10.17
AI Cru	12 06 07.687	-61 15 24.83	9.69
UX CVn	12 14 48.54	+36 38 49.3	13.10
RS CVn	13 10 36.908	+35 56 05.59	8.23
Alpha Cen	14 39 36.204	-60 50 08.23	-0.1
HD 132742	15 00 58.349	-08 31 08.19	4.95

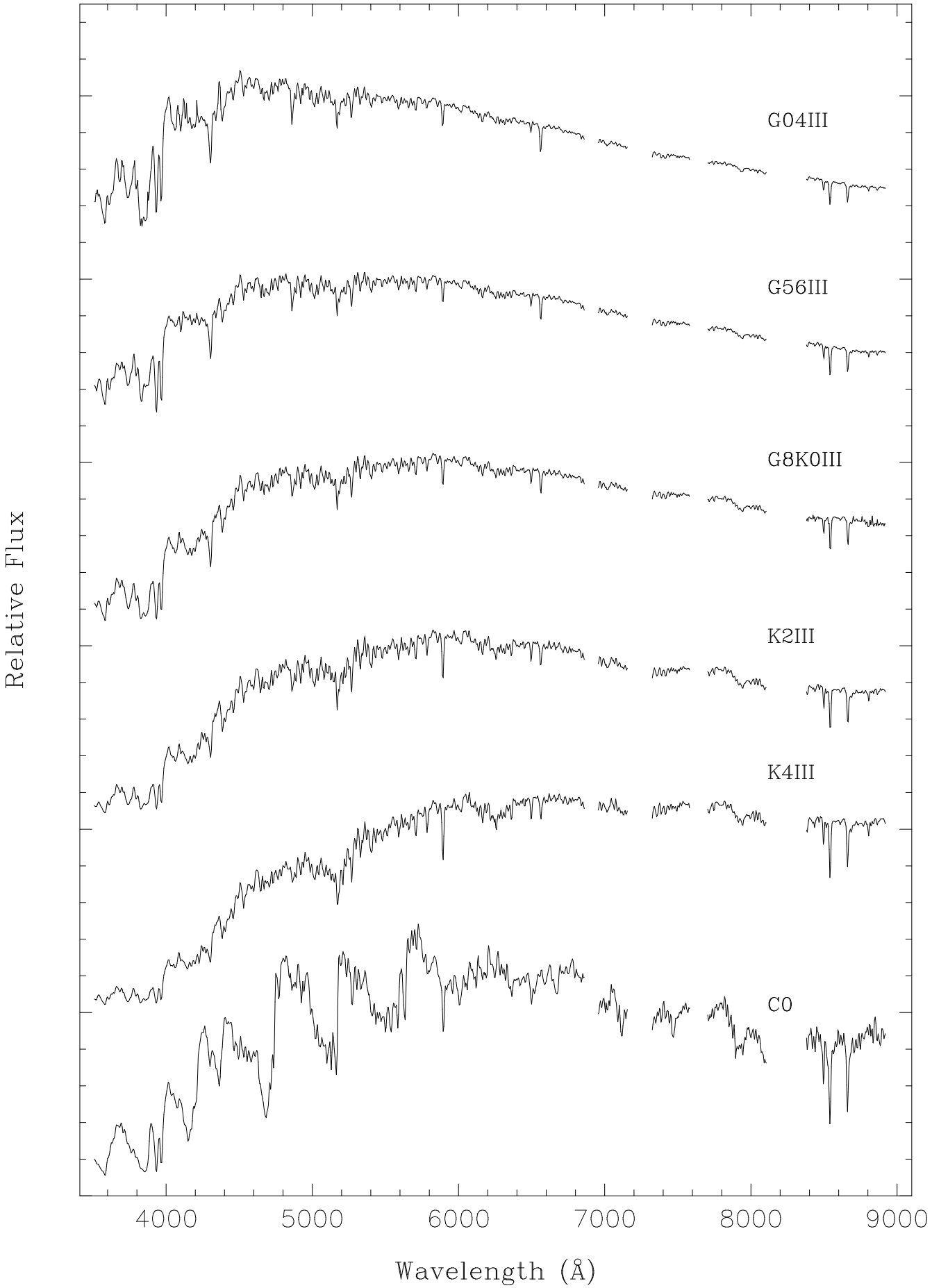
Object	RA(2000)	Dec(2000)	V
BD+48 2259	15 03 47.304	+47 39 14.62	4.76
UZ Lib	15 32 23.209	-08 32 00.91	9.11
Sco X-1	16 19 55.07	-15 38 25.0	12.2
V502 Oph	16 41 20.859	+00 30 27.37	8.53
AK Her	17 13 57.825	+16 21 00.61	8.51
V624 Her	17 44 17.247	+14 24 36.24	6.20
RS Sgr	18 17 36.245	-34 06 26.13	6.03
EG Ser	18 26 02.203	-01 40 51.42	8.24
RS Vul	19 17 39.991	+22 26 28.35	6.84
EM Cyg	19 38 40.12	+30 30 28.4	12.6
HD 191692	20 11 18.285	-00 49 17.26	3.24
V382 Cyg	20 18 47.220	+36 20 26.08	8.65
V836 Cyg	21 21 23.592	+35 44 10.61	8.76
DX Aqr	22 02 26.419	-16 57 52.39	6.37
HD 211416	22 18 30.094	-60 15 34.52	2.86
XZ Cep	22 32 25.080	+67 09 02.46	8.54
RT And	23 11 10.099	+53 01 33.04	9.03
AL Scl	23 55 16.587	-31 55 17.28	6.09
HD 222317	23 39 30.972	+28 14 47.42	6.97

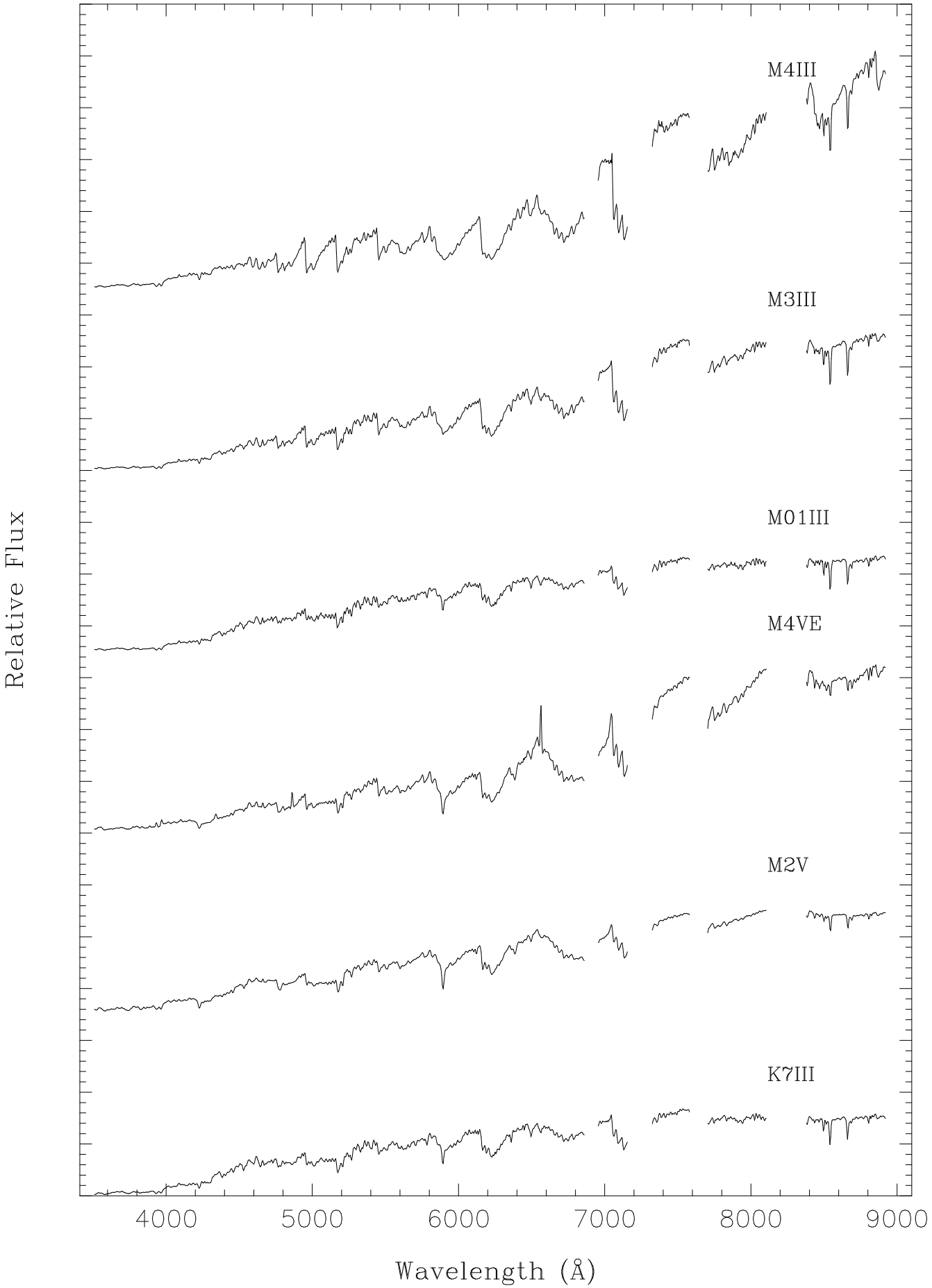

Relative Flux
O5V
O7B0V
B34V
B6V
A13V
A57V
A8V
A9F0V
4000
5000
6000
7000
8000
9000
Wavelength (Å)

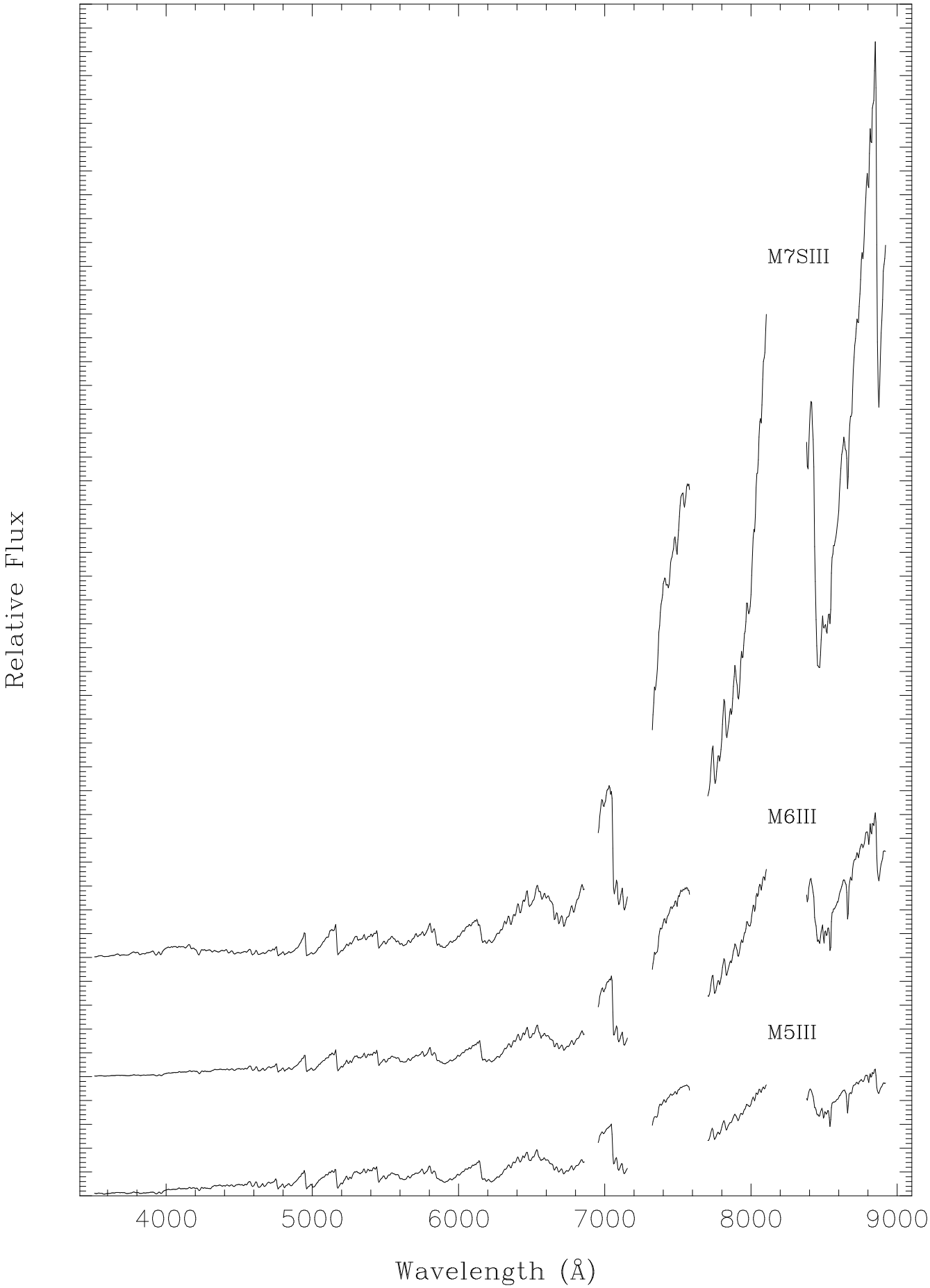

F67V
F89V
G12V
G68V
G9K0V
K4V
K5V
Relative Flux
4000
5000
6000
7000
8000
9000
Wavelength (Å)

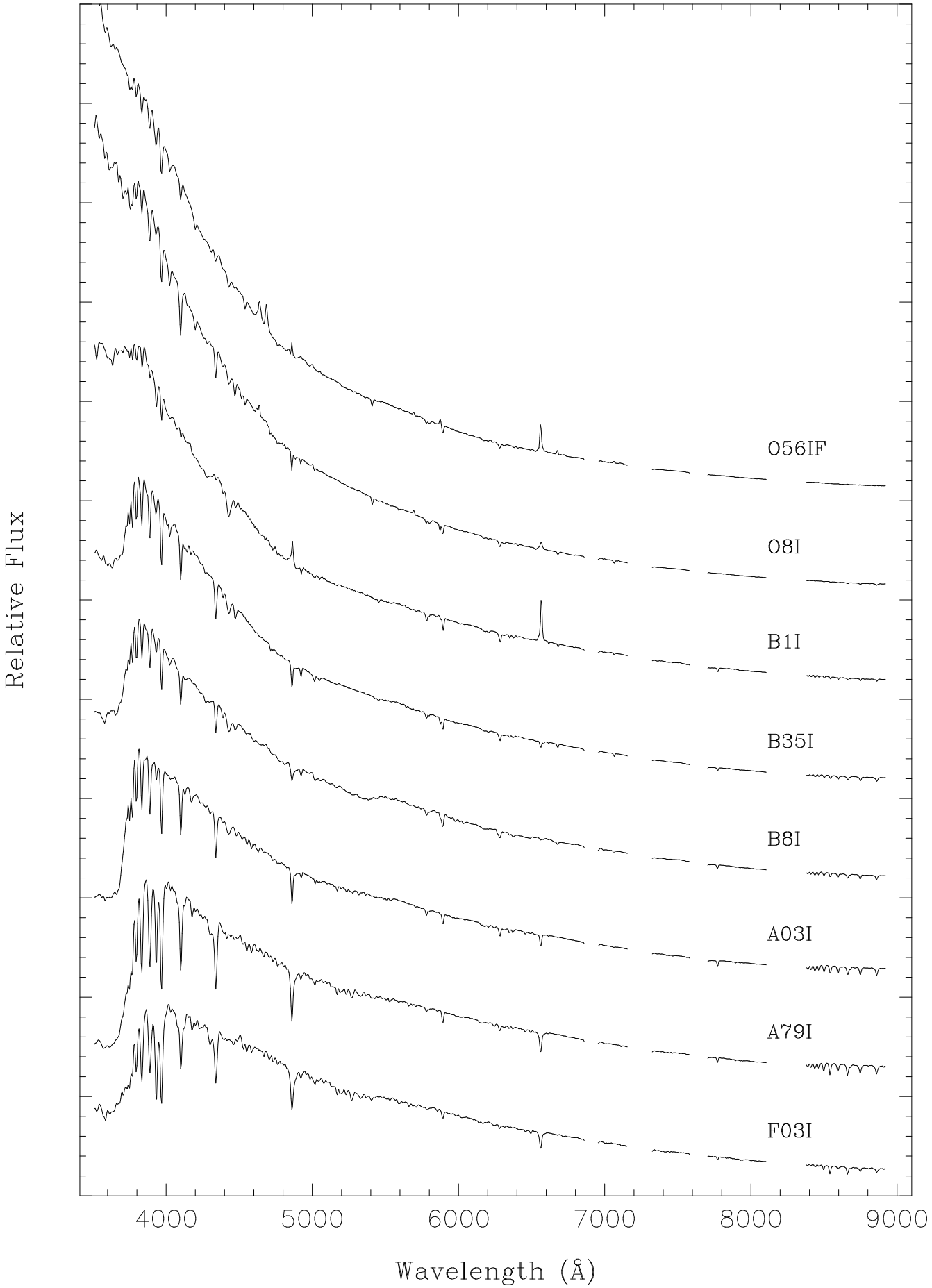

A7IV
F3IV
F89IV
G2IV
G5IV
G8IV
Relative Flux
4000
5000
6000
7000
8000
9000
Wavelength (Å)


Relative Flux
O7B1III
B5III
B9III
A3III
A6F0III
F47III
4000
5000
6000
7000
8000
9000
Wavelength (Å)


G04III
G56III
G8K0III
K2III
K4III
C0
Relative Flux
4000
5000
6000
7000
8000
9000
Wavelength (Å)


M4III
M3III
M01III
M4VE
M2V
K7III
Relative Flux
4000
5000
6000
7000
8000
9000
Wavelength (Å)


M7SIII
M6III
M5III
Relative Flux
4000
5000
6000
7000
8000
9000
Wavelength (Å)


O56IF
O8I
B1I
B35I
B8I
A03I
A79I
F03I
Relative Flux
4000
5000
6000
7000
8000
9000
Wavelength (Å)